completed in ~7 μs. The efficiency ϕ_{HT}' from the triplet complex to yield RO· and >ĊOH is large (~0.85) regardless of temperatures. Both RO· and >ĊOH produced by laser flash photolysis decay mainly via the radical recombination k_R between them with the rate constant 1.7×10^9 M^{-1} s^{-1}. The reaction mechanism for the hydrogen atom transfer reaction of ^{3}ROH* (produced by the triplet sensitization of BP) is shown in Schemes I and II.

Acknowledgment. The authors are very grateful to Professor P. J. Wagner of Michigan State University for his helpful suggestions and stimulating discussion.

Stereodynamics of a Series of Di-*tert*-butylphosphines [$(t\text{-}C_4H_9)_2PR$; R = H, CH_3, C_2H_5, $CH_2C_6H_5$, $i\text{-}C_3H_7$, $t\text{-}C_4H_9$, and C_6H_5]. Carbon-13, Proton, and Phosphorus-31 NMR Studies. Molecular Mechanics Calculations

Christopher D. Rithner* and C. Hackett Bushweller*

Contribution from the Department of Chemistry, University of Vermont, Burlington, Vermont 05405. *Received April 18, 1985*

Abstract: A series of di-*tert*-butylphosphines [$(t\text{-}C_4H_9)_2PR$; R = H, CH_3, C_2H_5, $CH_2C_6H_5$, $i\text{-}C_3H_7$, $t\text{-}C_4H_9$, and C_6H_5] has been studied by variable-temperature ^1H, $^{13}C\{^1H\}$, and $^{31}P\{^1H\}$ NMR spectroscopy. In all cases, the $^{31}P\{^1H\}$ spectrum remains a singlet down to 110 K. With the exception of $(t\text{-}C_4H_9)_2PH$, ^1H and $^{13}C\{^1H\}$ spectra show a decoalescence due to slowing *tert*-butyl rotation. For $(t\text{-}C_4H_9)_3P$, $^{13}C\{^1H\}$ spectra display two separate decoalescence phenomena over different temperature ranges. These are attributed to *tert*-butyl rotation ($\Delta G^\ddagger$ = 8.9 kcal/mol) and to libration of twisted *tert*-butyl groups ($\Delta G^\ddagger$ = 5.9 kcal/mol), which effects racemization of C_3-symmetric equilibrium enantiomers. The $^{13}C\{^1H\}$ spectrum of $(t\text{-}C_4H_9)_2P(i\text{-}C_3H_7)$ at 110 K reveals a strong preference for that conformation having one isopropyl methyl group oriented anti and the other gauche to the phosphorus lone pair, as well as a *tert*-butyl rotation barrier ($\Delta G^\ddagger$ = 6.7 kcal/mol) which is higher than the isopropyl rotation barrier ($\Delta G^\ddagger$ = 4 .8 kcal/mol). Both ^1H and $^{13}C\{^1H\}$ spectra of $(t\text{-}C_4H_9)_2PC_6H_5$ suggest an equilibrium conformation in which the phenyl plane bisects the CPC bond angle associated with the two *tert*-butyl groups, and the spectra also reveal a relatively high barrier to 2-fold phenyl rotation ($\Delta G^\ddagger$ = 10.5 kcal/mol) as compared to *tert*-butyl rotation ($\Delta G^\ddagger$ = 6.3 kcal/mol). For all seven phosphines, molecular mechanics calculations predict equilibrium conformations with twisted *tert*-butyl groups. For those phosphines in which R ≠ H, the molecular mechanics calculations also predict a twist about the P–R bond. The *tert*-butyl and P–R twisting result presumably from optimization of repulsions between proximate groups which are bonded to the ends of C–P–C linkages. For R = C_2H_5 and $CH_2C_6H_5$, the molecular mechanics calculations predict a strong preference of the C_2H_5 methyl and $CH_2C_6H_5$ phenyl groups for positions gauche and not anti to the lone pair. For all these phosphines, molecular mechanics predicts *tert*-butyl rotation barriers which are higher than libration (twisting) barriers. For R = CH_3, C_2H_5, $CH_2C_6H_5$, $i\text{-}C_3H_7$, and C_6H_5, the NMR spectrum recorded at the lowest temperature which allowed a meaningful spectrum (ca. 110 K) is consistent with *slow tert*-butyl rotation and *rapid* libration on the NMR time scale which agrees with molecular mechanics predictions of libration barriers too low to be NMR-accessible. For $(t\text{-}C_4H_9)_3P$, molecular mechanics predicts C_3-symmetric equilibrium enantiomers with both *tert*-butyl and libration barriers high enough to be NMR-accessible. $^{13}C\{^1H\}$ spectra show two decoalescence phenomena attributed to both processes.

Amines and phosphines constitute two important classes of chemical compounds which possess a tricoordinate, pyramidal central atom. In attempting to elucidate the stereodynamics of secondary or tertiary amines and phosphines, one must remain cognizant of pyramidal inversion at the tricoordinate center, isolated rotation about the bonds to nitrogen or phosphorus, and twisting about the bonds to the central atom in response to steric crowding.

In amines, the inversion barrier and pyramidality at nitrogen vary over a wide range and can be a function of N-substituent π-bonding, N-substituent electronegativity, steric crowding, and ring strain.[1] Nitrogen inversion barriers and isolated rotation barriers about carbon–nitrogen bonds can be comparable, and care must be taken in interpreting dynamic NMR (DNMR) spectra.[2,3] In contrast, inversion barriers in phosphines are high (>25 kcal/mol),[1,4] while isolated rotation barriers about carbon–phosphorus bonds are generally substantially lower. The rotation/inversion dichotomy in phosphines is clear-cut.[5-14]

(1) (a) Rauk, A.; Allen, L. C.; Mislow, K. *Angew. Chem., Int. Ed. Engl.* **1970**, *9*, 400. (b) Lambert, J. B. *Top. Stereochem.* **1971**, *6*, 19. (c) Raban, M.; Greenblatt, J. "The Chemistry of Amino, Nitroso, and Nitrocompounds and Their Derivatives"; Patai, S., Ed.; Wiley: New York, 1982; Part 1, pp 53–83.

(2) (a) Bushweller, C. H.; Fleischman, S. H.; Grady, G. L.; McGoff, P.; Rithner, C. D.; Whalon, M. R.; Brennan, J. G.; Marcantonio, R. P.; Domingue, R. P. *J. Am. Chem. Soc.* **1982**, *104*, 6224. (b) Fleischman, S. H.; Whalon, M. R.; Rithner, C. D.; Grady, G. L.; Bushweller, C. H. *Tetrahedron Lett.* **1982**, *23*, 4233.

(3) Bushweller, C. H.; Anderson, W. G.; Stevenson, P. E.; Burkey, D. L.; O'Neil, J. W. *J. Am. Chem. Soc.* **1974**, *96*, 3892.

(4) (a) Mislow, K. *Trans. N.Y. Acad. Sci.* **1973**, *35*, 227. (b) Baechler, R. D.; Mislow, K. *J. Am. Chem. Soc.* **1970**, *92*, 3090.

(5) (a) Kojima, T.; Breig, E. L.; Lin, C. C. *J. Chem. Phys.* **1961**, *35*, 2139. (b) Nelson, R. *Ibid.* **1963**, *39*, 2382. (c) Lide, D. R.; Cox, A. W., Jr. *Ibid.* **1976**, *64*, 1930.

(6) (a) Bartell, L. S. *J. Chem. Phys.* **1960**, *32*, 832. (b) Bartell, L. S.; Brockway, L. O. *Ibid.* **1960**, *32*, 512.

(7) (a) Durig, J. R.; Cox, A. W., Jr. *J. Chem. Phys.* **1975**, *63*, 2303. (b) Durig, J. R.; Cox, A. W., Jr. *Ibid.* **1976**, *80*, 2493. (c) Durig, J. R.; Cox, A. W., Jr. *J. Mol. Struct.* **1977**, *38*, 77.

(8) (a) Bushweller, C. H.; Brunelle, J. A. *J. Am. Chem. Soc.* **1973**, *95*, 5949. (b) Robert, J. B.; Roberts, J. D. *Ibid.* **1972**, *94*, 4902.

(9) (a) Bushweller, C. H.; Brunelle, J. A. *Tetrahedron Lett.* **1974**, *11*, 893. (b) Schmidbaur, H.; Blaschke, G.; Kohler, F. H. *Z. Naturforsch., B* **1977**, *32b*, 757. (c) Bushweller, C. H.; Lourandos, M. Z. *Inorg. Chem.* **1974**, *13*, 2514.

(10) Wroczynski, R. J.; Mislow, K. *J. Am. Chem. Soc.* **1979**, *101*, 3980.

(11) Bushweller, C. H.; Anderson, W. G.; Stevenson, P. E. O'Neil, J. W. *J. Am. Chem. Soc.* **1975**, *97*, 4338.

(12) (a) Seymour, S. J.; Jonas, T. *J. Magn. Reson.* **1972**, *8*, 376. (b) Seymour, S. J.; Jonas, J. *J. Chem. Phys.* **1971**, *54*, 487.

0002-7863/85/1505-7823$01.50/0

Sterically encumbered phosphines are now playing important roles as ligands in metal complexes which exhibit regioselective or enantioselective catalytic reactions. An understanding of the stereodynamics of the free phosphines can be useful in studying the metal–phosphine complexes. For example, in the encumbered tri-*tert*-butylphosphine, molecular mechanics and semiempirical molecular orbital calculations predict a C_3-symmetric, *chiral* equilibrium geometry,[15,16] and electron diffraction studies confirm these predictions.[17] In contrast, trimethylphosphine adopts an achiral C_{3v} equilibrium geometry.[7b] Chirality in the sterically crowded tri-*tert*-butylphosphine results from a twisting about the carbon–phosphorus bonds away from molecular geometries which have planes of symmetry. Presumably, the twisting results from an optimization of repulsive interactions between pairs of proximate *syn*-1,3-dimethyl groups.[18-20] Such chirality for the equilibrium geometry of tri-*tert*-butylphosphine complicates the energy surface for rotation about the carbon–phosphorus bonds. Two rate processes occur: (1) an essentially 3-fold *tert*-butyl *rotation* and (2) a *libration* or twisting process which involves a much smaller torsional amplitude than rotation.[21] While isolated rotation barriers about carbon–phosphorus bonds have been measured in many systems,[8-14] direct measurements of libration barriers are few.[10]

This paper concerns ^1H, $^{13}C\{^1H\}$, and $^{31}P\{^1H\}$ NMR studies of the series of di-*tert*-butylphosphines below (**1–7**). The NMR data in conjunction with molecular mechanics calculations (Allinger's 1980 MM2 force field)[22] allow us to propose a comprehensive

$(t\text{-}C_4H_9)_2PR$

1: R = H
2: R = CH_3
3: R = C_2H_5
4: R = $CH_2C_6H_5$
5: R = $i\text{-}C_3H_7$
6: R = $t\text{-}C_4H_9$
7: R = C_6H_5

picture of the stereodynamics of each of the seven phosphines including predictions of equilibrium conformations and itineraries for conformational exchange.

Results and Discussion

Di-*tert*-butylphosphine (1): The $^{13}C\{^1H\}$ NMR spectrum of **1** (10% v/v in vinyl chloride) at 262 K shows a doublet at δ 31.9 (tetramethylsilane (TMS) reference; CH_3; $^2J_{PC}$ = 13.0 Hz) and a doublet at δ 30.2 (quaternary carbon; $^1J_{PC}$ = 16.7 Hz). No decoalescence is observed down to 109 K (See Figure 1 in supplementary material). The ^1H NMR spectrum of **1** at 200 K shows a doublet at δ 1.20 (TMS reference; CH_3; $^3J_{PH}$ = 11.0 Hz) and a doublet at δ 3.06 (PH; $^1J_{PH}$ = 200.6 Hz). The $^{31}P\{^1H\}$ NMR spectrum of **1** at 260 K is a singlet at δ 19.9 (85% H_3PO_4 external reference). No decoalescence is observed in the ^1H and $^{31}P\{^1H\}$ spectra down to 110 K. It is apparent that all rotation barriers in **1** are too low to be DNMR-visible, and the three NMR studies above provide no incisive information regarding the stereodynamics of **1**.

Table I. Selected MM2 Structural Parameters for the Equilibrium Conformations of Di-*tert*-butylphosphine (**1**)[a]

parameter	conformation **9**	conformation **10**
dihedral angle, deg		
C3–P2–C7–C8	71.5	43.6
C4–C3–P2–C7	43.6	71.5
bond angle, deg		
C3–P2–C7	112.4	112.4
C3–P2–H11	97.6	99.4
C7–P2–H11	99.4	97.5
bond length, Å		
P2–C3	1.871	1.867
P2–C7	1.867	1.871
P2–H11	1.437	1.437

[a] See supplemental Table IS for a more comprehensive list of MM2 structural parameters.

The possibility that all the chemical shifts of diastereotopic methyl groups are identical in the equilibrium geometry of **1** (see **8a**) at 110 K is remote. For example, the ^1H NMR spectrum of *tert*-butyldichlorophosphine at 190 K is a doublet (δ 1.19; $^3J_{PH}$ = 15.5 Hz). At 115 K, the spectrum is decoalesced into one

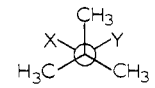

8a: X = H, Y = t-C_4H_9
8b: X = Y = Cl

doublet at δ 1.15 (6 H, $^3J_{PH}$ = 21.0 Hz; methyl groups which are gauche to lone pair; see **8b**) and another doublet at δ 1.26 (3 H, $^3J_{PH}$ = 4.5 Hz; anti methyl; see **8b**). This DNMR behavior is illustrated in Figure 2 in the supplementary material and clearly demonstrates not only different chemical shifts for methyl groups which are anti or gauche to the lone pair but also very different $^3J_{PH}$ values.[8] DNMR line-shape simulation gave the *tert*-butyl rotation barrier ($\Delta G^{\ddagger}$ = 6.7 ± 0.4 kcal/mol at 130 K).[24] This barrier is high enough to be DNMR-visible.

In order to provide some insight into the stereodynamics of **1**, molecular mechanics calculations were done by using Allinger's 1980 MM2 force field.[22] The parameters used for phosphorus(III) were developed previously for the MM1 force field and were used in the MM2 force field without any further optimization.[15] This transferral of parameters from one force field model to another could account for some of the small discrepancies between observed and calculated rotation barriers (vide infra). When the force field for phosphorus(III) is parameterized, the lone pair is not treated explicitly while other force fields for divalent oxygen and trivalent nitrogen do treat the lone pair(s) explicitly.[15,25] Heats of formation for phosphines cannot be calculated due to a lack of experimental data. Thus, we used the MM2-computed "steric energy" as a measure of relative conformer energy.[15] In searching for energy minima, a series of geometries corresponding to small, systematic torsions about a pertinent bond were input and allowed to relax fully by using the modified Newton–Rapshon minimization scheme.[22] If a particular conformation was found initially to occupy a local energy minimum, conformations with dihedral angles slightly different from those in that first-discovered min-

(13) (a) Rieker, A.; Kessler, H. *Tetrahedron Lett.* **1969**, 1227. (b) Bellamy, A. J.; Gould, R. O.; Walkinshaw, M. D. *J. Chem. Soc., Perkin Trans. 2* **1981**, 1099. (c) Negrebetskii, V. V.; Bokanov, A. I.; Bogel'fer, L. Y.; Rozcenel'skaya, N. A.; Stepanov, B. I. *J. General Chem. USSR* **1978**, *48*, 1308.

(14) Wille, E. E.; Stephenson, D. S.; Capriel, P.; Binsch, G. *J. Am. Chem. Soc.* **1982**, *104*, 405.

(15) Allinger, N. L.; Voithenberg, H. *Tetrahedron* **1978**, *34*, 627.

(16) Corosine, M.; Crasnier, F. *J. Mol. Struct.* **1975**, *27*, 105.

(17) Oberhammer, H.; Schmutzler, R.; Stelzer, O. *Inorg. Chem.* **1978**, *17*, 1254.

(18) Nachbar, R. B., Jr.; Johnson, C. A.; Mislow, K. *J. Org. Chem.* **1982**, *47*, 4829.

(19) (a) Burgi, H. B.; Bartell, L. S. *J. Am. Chem Soc.* **1972**, *94*, 5236. (b) Doun, S. K.; Bartell, L. S. *J. Mol. Struct.* **1980**, 63, 249.

(20) We define 1,3-dimethyl groups as methyl groups which are bonded, respectively, to the end atoms of a three-atom chain, e.g., CH_3–C–P–C–CH_3. For example, in di-*tert*-butylphosphine, a methyl group on one *tert*-butyl group is located 1,3 to any of the methyl groups on the *other tert*-butyl group.

(21) We define *rotation* as a torsional motion about a bond with a large change in the dihedral angle (e.g., 100° to 120°) between vicinal substituents *and* involving the *eclipsing of vicinal substituents* during the course of converting one rotamer to another. We define *libration* as a lower amplitude torsional motion about a bond (e.g., 10° to 40°) during which vicinal substituents do not eclipse, but during which pairs of proximate (syn) 1,3-substituents might undergo close passage. A 360° *tert*-butyl rotation will effect a complete site exchange for all three methyl groups, while *tert*-butyl libration *alone* will not effect a complete exchange. Rotation barriers are normally higher than libration barriers.

(22) Allinger, N. L.; Yuh, Y. H. *QCPE* **1980**, *395*. The parameters developed previously for phosphorus(III) were input at run time and used without any further optimization.[15]

(23) Reference deleted in proof.

(24) Computer program DNMR4 was used for the line-shape simulations. Bushweller, C. H.; Letendre, L. J.; Brunelle, J. A.; Bilofsky, H. S.; Whalon, M. R.; Fleischman, S. H. *QCPE* **1983**, *466*.

(25) Allinger, N. L. *Adv. Phys. Org. Chem.* **1976**, *13*, 1.

imum energy geometry were input, and minimization was allowed to occur again to ensure the accurate identification of an equilibrium geometry. We used the dihedral angle driver method rather than the restricted motion approach to compute rotation barriers and also as a second technique for discovering equilibrium geometries.[22]

The MM2 calculations predict two enantiomeric equilibrium geometries for **1** (see **9** and **10**). A perusal of selected MM2 structural parameters in Table I will indicate that **9** and **10** both have C_1 symmetry and are enantiomeric. A more complete

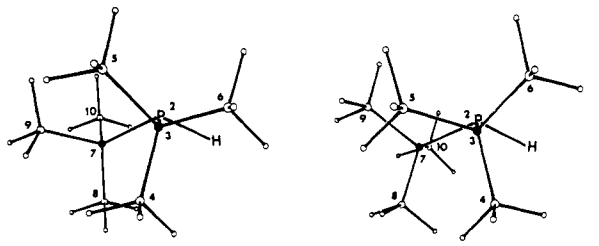

9

10

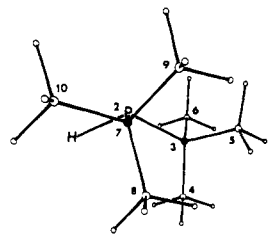

11

compilation of MM2 structural parameters can be found in supplemental Table IS. The geometric relationship between **9** and **10** may be more easily visualized by rotating **10** to give **11**. The enantiomeric relationship between **9** and **11** should now be apparent. Of course, **9** and **10** are computed to have identical steric energies. In **9**, the C3 and C7 *tert*-butyl groups are twisted clockwise (looking down the C–P bonds) approximately 10° and 20°, respectively, away from a molecular geometry having C_s symmetry and perfectly staggered *tert*-butyl groups. In **10**, the C7 and C3 *tert*-butyl groups are twisted counterclockwise 10° and 20°, respectively. For **9** and **10**, other structural parameters correlate (bond lengths, bond angles; Tables I and IS). The MM2 force field also predicts that individual methyl groups adopt essentially perfectly staggered orientations along C–CH_3 bonds in **1** and in the other posphines in this study (**2**–**7**). It is apparent that *tert*-butyl twisting in **9** and **10** alleviates *syn*-1,3-dimethyl repulsions which are at a maximum in a C_s-symmetric conformation.

A dihedral angle driver barrier calculation was performed for **1**. The energy profile resulting from 5° incremental changes in the dihedral angle C3–P2–C7–C8 (see **9**) with a counterclockwise torsion of the *tert*-butyl group (looking down the C7-P2 bond) is shown in Figure 3. The minima in Figure 3 correspond to **9** or **10**. The smaller maxima at or near −180°, −60°, 60°, and 180° reveal a low barrier (1.0 kcal/mol) separating **9** and **10**. This low barrier process is *libration* which involves small conrotatory torsions of *both tert*-butyl groups during which *syn*-1,3-dimethyl groups at C4 and C8 as well as C5 and C9 are in close passage. *No vicinal substituents eclipse each other during libration.*[21] Libration is sufficient to racemize **9** and **10**. Since both *tert*-butyl groups twist during libration and MM2 predicts that only one barrier is crossed (Figure 3), it is tempting to suggest that the libration transition state has C_s symmetry. The MM2-computed barrier (1.0 kcal/mol) is too low to be DNMR-visible.

In Figure 3, the higher maxima near dihedral angles −120°, 0°, and 120° are due to *tert*-butyl *rotation*. An examination of Figure 3 suggests that a direct *tert*-butyl rotation with no prior libration will also racemize **9** and **10**. Starting from **10**, a 44°

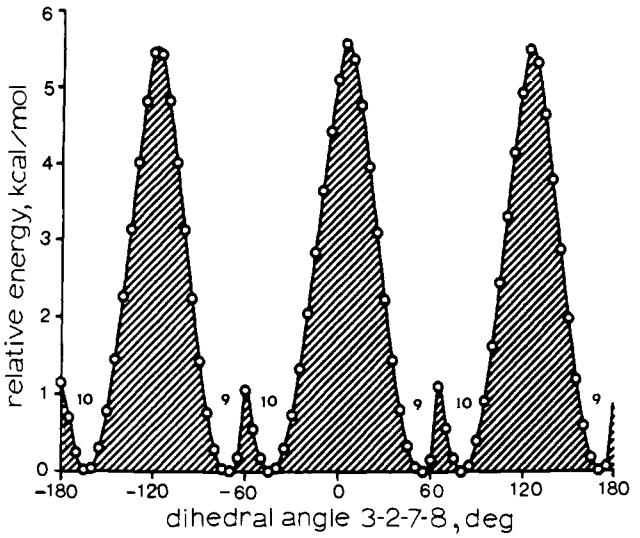

Figure 3. Energy profile derived from an MM2 dihedral angle driver calculation for di-*tert*-butylphosphine (**1**). Dihedral angle C3–P2–C7–C8 (**9**) is changed in 5° counterclockwise increments looking down the C7–P2 bond.

counterclockwise torsion about the C7–P2 bond will produce a geometry having C8/*tert*-butyl, C9/lone pair and C10/PH *vicinal eclipsings* (Figure 3; dihedral angle C3–P2–C7–C8 = 0°). This is the transition state for *tert*-butyl rotation with an MM2-computed barrier of 5.6 kcal/mol. If the counterclockwise rotation about the C7–P2 bond continues beyond the eclipsed transition state and the other *tert*-butyl group remains in its initial position in **10**, a conformation with C_s symmetry is encountered. This geometry has two pairs of *syn*-1,3-dimethyl repulsions which are relieved by a slight *clockwise* torsion about the C3–P2 bond to ultimately produce **9**. Thus, rotation of one *tert*-butyl group in conjunction with a small disrotatory torsion of the other *tert*-butyl group effects racemization. Of course, racemization can also occur via a much lower barrier libration. *It is noteworthy that both libration and rotation involve geometrical reorientations across the whole molecular system. Rotation or libration of a tert-butyl group is not a single, locally isolated process.*

In addition, we found no indication in the MM2 calculations for a concomitant *rotation* of both *tert*-butyl groups (i.e., gearing) as a reasonable itinerary for *tert*-butyl rotation.[26] It is apparent that one *tert*-butyl group rotates at a time in conjunction with a low-amplitude, disrotatory torsion of the other group.

The MM2-computed *tert*-butyl rotation barrier (5.6 kcal/mol) is within the DNMR-visible range. However, the NMR studies (vide supra) reveal a barrier which is less than 5 kcal/mol. Indeed, it is clear that both *tert*-butyl rotation and libration barriers are too low to be DNMR-visible.

The stereodynamics of **1** suggested by the MM2 calculations resembles that of other phosphines in this report. Equilibrium conformations have twisted alkyl or aryl substituents and reduced molecular symmetry due to 1,3-repulsions between pertinent groups. Barriers to *tert*-butyl rotation are consistently higher than barriers to libration. A compilation of rotation and libration barriers computed by using the MM2 force field and measured by using the DNMR method can be found in Table II.

The C_1 symmetry of **9** or **10** renders *all* the methyl groups diastereotropic. Under conditions of slow *tert*-butyl rotation *and* libration on the NMR time scale, the chemical shifts of the methyl groups would all be, in principle, anisochronous in the ^1H and $^{13}C\{^1H\}$ NMR spectra. Therefore, if the *tert*-butyl rotation barrier is higher than the libration barrier, both processes should be DNMR-visible *for symmetry reasons*. However, the NMR studies for **1** reported above reveal that both processes have barriers too low to be DNMR-visible.

(26) Johnson, C. A.; Guenzi, A.; Nachbar, R. B., Jr.; Blount, J. F.; Wennerström, O.; Mislow, K. *J. Am. Chem. Soc.* **1982**, *104*, 5163.

Table II. Rotation and Libration Barriers

compd	most stable conformations	process	MM2 barrier kcal/mol	DNMR barrier $\Delta G^{\ddagger}$, kcal/mol (temp K)
1	**9**, **10**	**9** to **10** libration	1.0	
		t-C_4H_9 rotation	5.6	
2	**12**, **13**	**12** to **13** libration	1.3	
		t-C_4H_9 rotation	7.4	6.2 ± 0.3 (120)
3	**15**, **16**	**15** to **17** libration	2.3	
		19 to **20** libration	2.9	
		15 to **16** rotation	2.0	
		17 to **19** rotation	7.4	
		t-C_4H_9 rotation[a]	7.8	6.4 ± 0.3 (137)
4	**23**, **24**	**21** to **23** libration	1.2	
		25 to **26** libration	0.5	
		21 to **22** rotation	3.9	
		23 to **25** rotation	7.8	
		t-C_4H_9 rotation[b]	7.7	6.2 ± 0.3 (128)
5	**29**, **30**	**29** to **27** libration	3.7	
		31 to **32** libration	1.3	
		27 to **28** rotation	14.3	
		29 to **31** rotation	5.9	4.8 ± 0.5 (110)
		t-C_4H_9 rotation[c]	8.9	6.7 ± 0.3 (138)[e]
		t-C_4H_9 rotation[d]	8.0	
6	**33**, **34**	**33** to **34** libration	6.1	5.9 ± 0.4 (124)
		t-C_4H_9 rotation	9.9	8.9 ± 0.4 (180)
7	**36**, **37**	**36** to **37** libration[f]	1.0	
		t-C_4H_9 rotation	7.0	6.3 ± 0.4 (140)
		C_6H_5 rotation	14.0	10.5 ± 0.3 (228)

[a] C7 t-C_4H_9 of **15**. [b] C7 t-C_4H_9 of **21**. [c] C7 t-C_4H_9 of **29**. [d] C3 t-C_4H_9 of **29**. [e] Measured under conditions of rapid i-C_3H_7 rotation. [f] t-C_4H_9 driver calculation.

Di-*tert*-butylmethylphosphine (2). The ^1H NMR spectrum (270 MHz) of **2** (10% v/v in vinyl chloride) at 200 K consists of doublets at δ 1.07 (t-C_4H_9; $^3J_{PH}$ = 10.3 Hz) and at δ 0.90 (PCH_3; $^2J_{PH}$ = 3.7 Hz) as shown in Figure 4. At lower temperatures, the P-methyl doublet undergoes no decoalescence although T_2 broadening coalesces the doublet. The *tert*-butyl resonance is decoalesced at 110 K into *three* signals of equal area at δ 1.19 ($^3J_{PH}$ = 13.5 Hz), δ 1.07 ($^3J_{PH}$ = 4.5 Hz), and δ 0.93 ($^3J_{PH}$ = 13.0 Hz). The T_2-broadened P-methyl signal is superimposed on the upfield component of the doublet at δ 0.93. Although the resonance at δ 1.07 appears as a broad singlet, the $^3J_{PH}$ value of 4.5 Hz in conjunction with a short T_2 value and a small exchange rate is required to obtain an internally consistent fit of the whole spectrum. Consistent with previous studies, the signals at δ 1.19 and 0.93 with relatively large $^3J_{PH}$ values are assigned to methyls which are gauche to the lone pair and the peak at δ 1.07 (small $^3J_{PH}$) to the methyl which is anti to the lone pair.[8] The 110 K spectrum is consistent with slow *tert*-butyl rotation.[8] The signals for all methyl groups were simulated effectively at 110 K as three homotopic protons; i.e., all individual methyl rotations about P-CH_3 and C-CH_3 bonds are fast on the NMR time scale at 110 K. From a three-site DNMR simulation at 120 K, the observed *tert*-butyl rotation barrier ($\Delta G^{\ddagger}$) is 6.2 ± 0.3 kcal/mol.

The $^{13}C\{^1H\}$ NMR spectrum (62.9 MHz) of **2** (10% v/v in vinyl chloride) at 260 K shows doublets at δ 29.5 (t-C_4H_9 methyls; $^2J_{PC}$ = 14.1 Hz), δ 30.5 (quaternary; $^1J_{PC}$ = 21.0 Hz), and δ 4.5 (PCH_3; $^1J_{PC}$ = 19.3 Hz). The P-methyl and quaternary carbons resonances undergo no decoalescence down to 113 K. The *tert*-butyl methyl's resonance is decoalesced at 113 K into *three* signals of equal area at δ 31.5 ($^2J_{PC}$ = 23.0 Hz), δ 30.6 ($^2J_{PC}$ = 17.0 Hz), and δ 24.3 ($^2J_{PC}$ = 4 Hz). This DNMR behavior and the theoretical decomposition of a simulation of the 113 K spectrum are illustrated in Figure 5 and 6 of the supplementary material. The two signals at δ 31.5 and 30.6 with larger $^2J_{PC}$ values are assigned to methyl groups which are gauche to the lone pair, while the resonance at δ 24.3 ($^2J_{PC}$ = 4 Hz) is assigned to the anti methyl. *tert*-Butyl rotation is slow at 113 K. From a three-site DNMR simulation at 138 K, the observed *tert*-butyl rotation barrier ($\Delta G^{\ddagger}$) is 6.5 ± 0.4 kcal/mol.

Both the ^1H and $^{13}C\{^1H\}$ spectra of **2** at about 110 K reveal slow *tert*-butyl rotation. The observation of just *three tert*-butyl methyl signals at 110 K suggests C_s molecular symmetry. In light of the MM2 calculations for **1** which show twisted *tert*-butyl groups and C_1 symmetry for the enantiomeric equilibrium conformations (**9**; **10**), it is apparent that the C_s symmetry suggested by the NMR spectrum of **2** at 110 K is time-averaged; i.e., *tert*-butyl rotation is slow on the NMR time scale while libration remains fast.

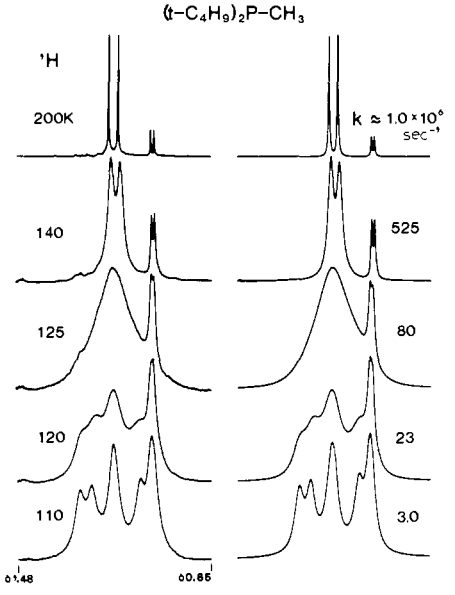

Figure 4. Experimental ^1H DNMR spectra (270 MHz; left column) of di-*tert*-butylmethylphosphine (**2**; 10% v/v in vinyl chloride) and theoretical simulations as a function of the rate of *tert*-butyl rotation (right column; k is the first-order rate constant for conversion of one *tert*-butyl rotamer to one other).[24]

The $^{31}P\{^1H\}$ NMR spectrum (101.2 MHz) of **2** (10% v/v in vinyl chloride) is a singlet (δ 10.8) at 260 K and remains a singlet down to 110 K.

In light of the fact that the ^1H and $^{13}C\{^1H\}$ spectra of **2** at 110 K suggest a molecular symmetry higher than C_1, we pursued MM2 calculations. The results are analogous to those for di-*tert*-butylphosphine (**1**). The MM2 force field predicts two enantiomeric equilibrium geometries (C_1 symmetry) for **2** (see **12** and **13**). Selected MM2 structural parameters can be found in Table III and a more comprehensive compilation in supplemental Table IS.

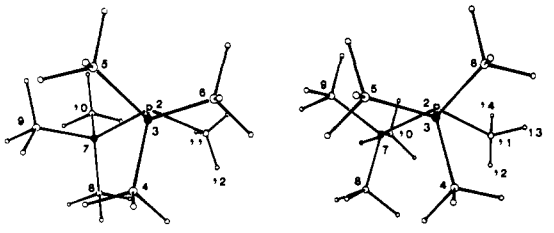

12 **13**

The MM2 prediction of enantiomeric equilibrium geometries for **2** which have C_1 symmetry supports the rationale that the ^1H and $^{13}C\{^1H\}$ spectra at 110 K reflect a *time*-averaged C_s symmetry resulting from rapid libration. With slow *tert*-butyl rotation and slow libration, it would be possible in principle to observe six NMR signals for the six diastereotropic *tert*-butyl methyl groups (**12** or **13**). This is clearly not the situation at 110 K (Figures 4–6). However, if *tert*-butyl rotation is slow on the NMR time scale and libration is fast (i.e., the **12** to **13** process is fast), there will occur respective pairwise averagings of the ^1H or $^{13}C\{^1H\}$ chemical shifts of the C4 and C8 methyls, C5 and C9 methyls, and C6 and C10 methyls (**12**/**13**). Under these conditions, the NMR spectrum of the *tert*-butyl methyls will reduce to three signals as observed at 110 K (Figures 4–6) and will reflect time-averaged C_s symmetry.

A C3–P2–C7–C8 dihedral angle driver calculation for **2** gave an energy profile analogous to Figure 3 except that the maxima for **2** are at slightly higher energies. The MM2-computed barrier to libration is 1.3 kcal/mol which is well below the DNMR-visible limit. Libration will racemize **12** and **13**, and rapid libration with no *tert*-butyl rotation will reflect time-averaged C_s symmetry in the ^1H and $^{13}C\{^1H\}$ NMR spectra. **12** and **13** can also be racemized via *tert*-butyl rotation. A 97° clockwise rotation about the C3–P2 bond of **12** places C4 of **12** at position C5 in **13**, while the C7 *tert*-butyl and P-methyl groups undergo counterclockwise torsions to ultimately give **13**. The MM2-computed *tert*-butyl rotation barrier is 7.4 kcal/mol.

Thus, the DNMR-visible barrier in **2** is *tert*-butyl rotation with the libration barrier too low to be DNMR-accessible. This is qualitatively consistent with the MM2 barriers to *tert*-butyl rotation (7.4 kcal/mol) and libration (1.3 kcal/mol), but it should be noted that the MM2 *tert*-butyl rotation barrier is 1.2 kcal/mol higher than the DNMR barrier ($\Delta G^{\ddagger}$ = 6.2 kcal/mol).

Di-*tert*-butylethylphosphine (3). The ^1H NMR spectrum of **3** (10% v/v in vinyl chloride) at 204 K shows a doublet at δ 1.09 (t-C_4H_9; $^3J_{PH}$ = 9.8 Hz) and the A_2B_3 portion of an A_2B_3X spin system (CH_3CH_2P; X = ^{31}P; δ_A 1.32, δ_B 1.13, $^3J_{AB}$ = 7.8, $^2J_{AX}$ = 4.5, $^3J_{BX}$ = 16.5 Hz) as shown in Figure 7. Below 150 K, the *tert*-butyl resonance decoalesces and, at 119 K, is separated into three signals. *tert*-Butyl rotation is slow at 119 K. The A_2B_3X ethyl subspectrum undergoes no decoalescence down to 119 K (Figure 7) which indicates rapid rotation about the P–CH_2 bond even at 119 K. The details of this DNMR behavior are not immediately evident from a visual examination of the experimental spectra in Figure 7 but are determined by theoretical simulation.[24] A decomposition of the theoretical simulation of the 119 K spectrum (Figure 8) clearly shows just *three tert*-butyl resonances at δ 1.19 ($^3J_{PH}$ = 13.4 Hz), δ 1.10 ($^3J_{PH} \simeq$ 3.5 Hz), and δ 0.96 ($^3J_{PH}$ = 16.1 Hz). The signals at δ 1.19 and 0.96 with the larger $^3J_{PH}$ values are assigned to methyls which are gauche to the lone pair and the δ 1.10 resonance to the methyl which is anti to the lone pair (**14**).

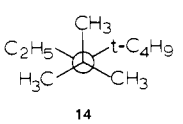

14

Although the P–ethyl subspectrum undergoes no decoalescence, the ^1H NMR spectrum at 119 K does provide evidence for a strong preference for rotamers which have the P–ethyl methyl group gauche to the lone pair. The large $^3J_{PH}$ value for the P–ethyl

Table III. Selected MM2 Structural Parameters for the Equilibrium Conformations of Di-*tert*-butylmethylphosphine (**2**)[a]

parameter	conformation **12**	conformation **13**
dihedral angle, deg		
C3–P2–C7–C8	71.7	44.0
C4–C3–P2–C7	43.6	71.5
C3–P2–C11–H12	50.9	68.0
bond angle, deg		
C3–P2–C7	113.4	113.5
C3–P2–C11	104.4	103.0
C7–P2–C11	103.0	104.4
bond length, Å		
P2–C3	1.848	1.851
P2–C7	1.851	1.848
P2–C11	1.832	1.832

[a] See supplemental Table IS for a more comprehensive list of MM2 structural parameters.

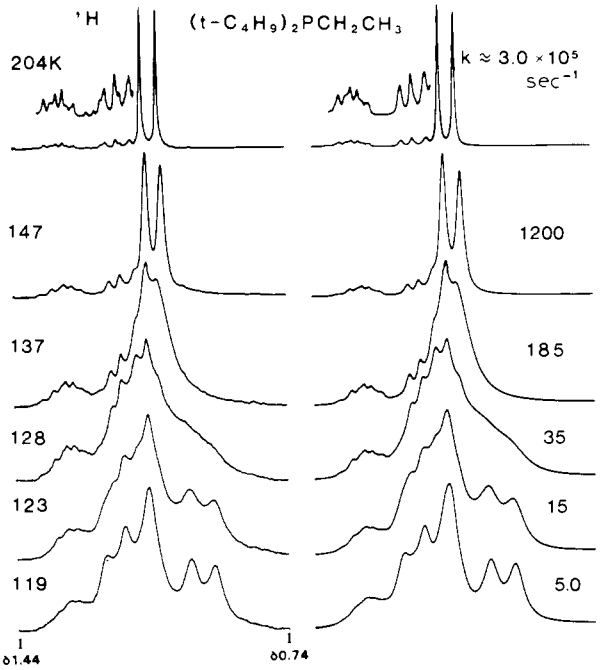

Figure 7. Experimental ^1H DNMR spectra (250 MHz; left column) of di-*tert*-butylethylphosphine (**3**; 10% v/v in vinyl chloride) and theoretical simulations as a function of the rate of *tert*-butyl rotation (right column; k is defined in the Figure 4 caption).

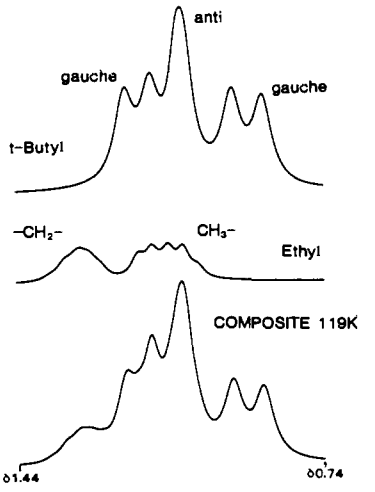

Figure 8. Decomposition of the theoretical simulation of the ^1H NMR spectrum of di-*tert*-butylethylphosphine (**3**) at 119 K. The top subspectrum is due to the *tert*-butyl group and the middle subspectrum to the ethyl group.

Table IV. Selected MM2 Structural Parameters for the Equilibrium Conformations of Di-*tert*-butylethylphosphine (**3**)[a]

parameter	conformation					
	15	**16**	**17**	**18**	**19**	**20**
dihedral angle, deg						
C4–C3–P2–C7	42.8	71.3	76.8	47.4	46.1	75.0
C3–P2–C7–C8	71.4	42.8	47.4	76.8	75.0	46.0
C3–P2–C11–C12	91.1	149.9	64.5	176.7	48.4	77.1
C7–P2–C11–C12	150.0	91.2	176.6	64.4	77.0	48.3
bond angle, deg						
C3–P2–C7	112.7	112.7	112.6	112.6	114.8	114.8
C3–P2–C11	106.3	103.3	106.4	103.5	109.2	107.8
C7–P2–C11	103.3	106.3	103.5	106.4	107.8	109.3
bond length, Å						
P2–C3	1.849	1.854	1.851	1.856	1.838	1.843
P2–C7	1.854	1.849	1.856	1.851	1.843	1.838
P2–C11	1.838	1.838	1.840	1.840	1.829	1.829

[a] See supplemental Table IIS for a more comprehensive list of MM2 structural parameters.

Table V. Relative MM2 Steric Energies for Equilibrium Conformations

compd	conformation	rel steric energy, kcal/mol
3	**15**, **16**[a]	0.00
	17, **18**	0.19
	19, **20**	1.60
4	**21**, **22**[a]	0.00
	23, **24**	0.04
	25, **26**	4.24
5	**29**, **30**[a]	0.00
	27, **28**	1.21
	31, **32**	3.52

[a] Most stable equilibrium conformation.

methyl group (16.5 Hz) is consistent with a strong preference of methyl for positions gauche to the lone pair.[8] $^3J_{PH}$ values for methyl anti to the lone pair are much smaller (3–4 Hz).[8] Thus, it is apparent that the ethyl group is interconverting rapidly and exclusively at 119 K between the two positions gauche to the lone pair. This process is sufficient to interchange the methylene protons chemical shifts and give an A_2B_3X subspectrum. The 119 K spectrum reflects time-averaged C_s symmetry and is consistent with *slow-tert*-butyl rotation, *fast* rotation about the P–CH_2 bond, and *fast* libration on the NMR time scale. From a DNMR simulation at 137 K, the *tert*-butyl rotation barrier ($\Delta G^{\ddagger}$) is 6.4 ± 0.3 kcal/mol.

The $^{13}C\{^1H\}$ NMR spectrum (62.9 MHz) of **3** (10% v/v in vinyl chloride) at 195 K shows doublets at δ 29.6 (*t*-C_4H_9 methyls; $^2J_{PC}$ = 13.0 Hz), δ 31.5 (quaternary carbon; $^1J_{PC}$ = 22.2 Hz), δ 15.4 (C_2H_5 methyl; $^2J_{PC}$ = 27.8 Hz), and δ 14.2 (CH_2; $^1J_{PC}$ = 20.4 Hz). Below 195 K, the ethyl and quaternary carbons resonances undergo no decoalescence, while the *tert*-butyl methyls signal does decoalesce (see Figure 9 in supplementary material). As shown in the decomposition of the theoretical simulation of the 119 K spectrum (see Figure 10 in supplementary material), the *tert*-butyl methyls give three resonances at δ 31.9 ($^2J_{PC}$ = 16.1 Hz; gauche to lone pair), δ 31.0 ($^2J_{PC}$ = 22.0 Hz; gauche to lone pair), and δ 25.1 ($^2J_{PC} \cong$ 5 Hz; anti to lone pair; doublet coalesced due to T_2 broadening). The DNMR-visible process is *tert*-butyl rotation with a barrier ($\Delta G^{\ddagger}$) of 6.4 ± 0.3 kcal/mol at 138 K in good agreement with the ^1H value.

Consistent with the ^1H DNMR spectra, the $^{13}C\{^1H\}$ spectra show that rotation about the P–CH_2 bond is fast at 119 K. The $^2J_{PC}$ value (25.3 Hz) for methyl of the ethyl group is more comparable to the $^2J_{PC}$ values for *tert*-butyl methyls which are gauche to the lone pair (16–23 Hz) rather than anti (4–5 Hz). Thus, it would appear from both $^3J_{PH}$ and $^2J_{PC}$ values that the ethyl group prefers positions gauche to the lone pair.

The $^{31}P\{^1H\}$ NMR spectrum (101.2 MHz) of **3** (10% v/v in vinyl chloride) at 262 K is a singlet (δ 33.7) and remains a singlet down to 113 K.

MM2 force field calculations predict substantially more complex stereodynamics for **3** than for **1** and **2**. For **3**, six chiral equilibrium geometries are predicted (**15**–**20**). A perusal of selected MM2 structural parameters in Table IV will reveal that **15**, **17**, and **19** are diastereomeric as are **16**, **18**, and **20**. There are three pairs

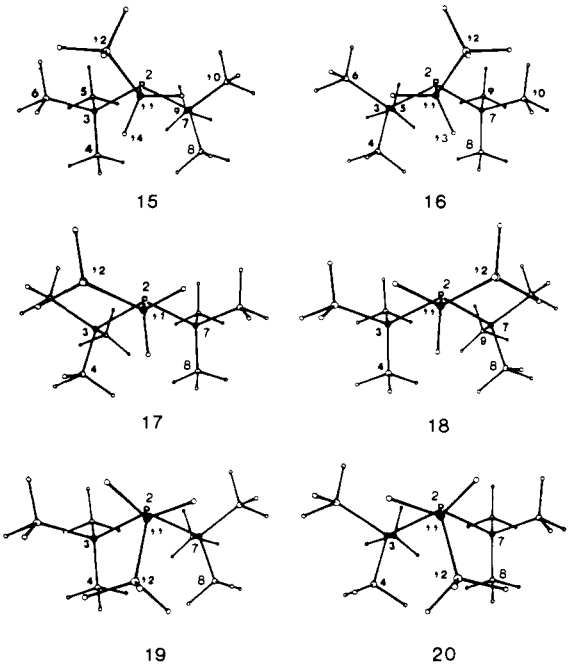

of enantiomers (**15** and **16**; **17** and **18**; **19** and **20**). A more comprehensive compilation of MM2 structural parameters can be found in supplemental Table IIS.

The MM2 force field predicts enantiomers **15** and **16** to be most stable, while **17** and **18** are only 0.09 kcal/mol less stable. The greater stability of **15** over **17** is due presumably to a reflief of the C6/C12 1,3-dimethyl repulsion, resulting from twisting the ethyl group toward the lone pair. It is noteworthy that the *tert*-butyl groups of **15** are also twisted in response to 1,3-dimethyl repulsions. Conformer **19** (or **20**) is 1.60 kcal/mol less stable than **15**, reflecting an additional 1,3-dimethyl repulsion for the anti ethyl group and a generally more crowded environment. A compilation of MM2 relative conformer energies for those phosphines (**3**–**5**) which adopt diastereomeric equilibrium conformations can be found in Table V.

Assuming no entropy difference between diastereomeric conformers and assuming the difference in steric energies to be a measure of enthalpy difference, the percentages of **15**–**16** (70%), **17**–**18** (30%), and **19**–**20** (0.03%) at 119 K indicate that **15**–**18** will be present at concentrations high enough to be NMR-detectable but **19**–**20** will clearly not be NMR-detectable. This is consistent with the large $^3J_{PH}$ and $^2J_{PC}$ values for methyl of the ethyl group (vide supra) which indicate a strong preference of the ethyl methyl group for positions gauche to the lone pair.

The four NMR-detectable conformers (**15**–**18**) all possess C_1 symmetry. However, the ^1H and $^{13}C\{^1H\}$ spectra at 119 K (Figures

Table VI. Selected MM2 Structural Parameters for the Equilibrium Conformation of Di-*tert*-butylbenzylphosphine (**4**)[a]

parameter	conformation					
	21[b]	**22**[c]	**23**[b]	**24**[c]	**25**[c]	**26**[b]
dihedral angle, deg						
C3–P2–C7–C8	73.4	45.0	45.7	73.5	45.6	67.6
C4–C3–P2–C7	45.0	73.4	73.4	45.8	67.8	45.9
C3–P2–C11–C12	74.2	166.6	66.7	173.1	54.4	73.4
C7–P2–C11–C12	166.8	74.5	174.0	67.6	74.0	54.9
P2–C11–C12–C15	132.8	48.3	123.2	57.1	80.2	100.9
P2–C11–C12–C16	48.3	132.9	57.5	123.7	101.1	80.4
bond angle, deg						
C3–P2–C7	113.0	113.0	113.0	113.0	115.1	115.1
C3–P2–C11	106.3	102.7	105.3	104.6	109.4	111.2
C7–P2–C11	102.7	106.3	104.5	105.2	111.2	109.4
bond length, Å						
P2–C3	1.848	1.854	1.852	1.851	1.841	1.836
P2–C7	1.854	1.847	1.851	1.852	1.836	1.840
P2–C11	1.837	1.837	1.837	1.837	1.826	1.826

[a] See supplemental Table IIIS for a more comprehensive list of MM2 structural parameters. [b] C15 is twisted toward reader. [c] C16 is twisted toward reader.

7–10) suggest a higher symmetry (C_s) and show no evidence of diastereomeric species. Dihedral angle driver barrier calculations for both the ethyl (angle C7–P2–C11–C12) and *tert*-butyl groups (angle C3–P2–C7–C8) shed light on the situation (Table I). The MM2 barriers for pure libration processes are all low and DNMR-invisible, i.e., **15** to **17** (2.3 kcal/mol) and **19** to **20** (2.9 kcal/mol). The barrier associated with a process involving P–ethyl *rotation* can vary significantly. The **15**-to-**16** barrier is very low (2.0 kcal/mol) while the **17**-to-**19** barrier is much higher (7.4 kcal/mol). A counterclockwise *rotation* of the C7 *tert*-butyl of **16** in in conjunction with small clockwise torsions of the C3 *tert*-butyl and ethyl groups converts **16** directly into **18**. The MM2 barrier for this *tert*-butyl rotation is a DNMR-visible 7.8 kcal/mol. For C3 *tert*-butyl rotation, the MM2 barrier is also a DNMR-visible 7.8 kcal/mol. The data in Table IV will show that the dihedral angle C7–P2–C11–C12 associated with the ethyl group is a unique descriptor for all the conformations **15–20**. As the C7–P2–C11–C12 dihedral angle changes, other unique geometric reorientations occur across the whole molecule. Thus, tracking this dihedral angle tracks exchange among all the equilibrium geometries of **3**. Using the MM2-computed steric energies and the MM2 barriers for conformational exchange among **15–20**, we constructed a summary energy profile by using the C7–P2–C11–C12 dihedral angle as the unique geometric descriptor (Chart I). It is evident that the four NMR-detectable conformations (**15–18**) can exchange among themselves via a series of low, DNMR-invisible barriers *without involving any tert-butyl rotation.* It is also apparent that the preferred exchange itinerary is the **17** to **15** to **16** to **18** route (and vice versa) with no direct exchange between **17** and **18**. Any exchange via **19** and **20** as intermediates involves much higher barriers and is disfavored. Thus, the ^1H and $^{13}C\{^1H\}$ spectra of **3** at 119 K reflect a family of four conformers (**15–18**) undergoing *rapid* intrafamily exchange (Chart I), while *tert*-butyl rotation is *slow* on the NMR time scale. The time-averaged symmetry of this exchanging system is C_s, and this is consistent with the spectra at 119 K (Figures 7–10).

Di-*tert*-butylbenzylphosphine (4). The ^1H and $^{13}C\{^1H\}$ NMR signals for the methyl groups of **4** (5% v/v in vinyl chloride) decoalescence at temperatures below 160 K. At 123 K, the methyl groups give the familiar three ^1H NMR signals at δ 1.20 ($^3J_{PH}$ = 4 Hz), δ 1.20 ($^3J_{PH}$ = 12 Hz), and δ 0.86 ($^3J_{PH}$ = 15 Hz). At 124 K, the methyl groups also give three $^{13}C\{^1H\}$ signals at δ 25.2 ($^2J_{PC} \simeq$ 4.5 Hz; anti CH_3), δ 30.9 ($^2J_{PC}$ = 20 Hz; gauche CH_3) and δ 31.9 ($^2J_{PC}$ = 14 Hz; gauche CH_3). *No other resonances decoalesce.* The $^{13}C\{^1H\}$ DNMR spectra are illustrated in Figure 11 in the supplementary material, and the 124 K spectrum is decomposed in Figure 12 in the supplementary material. The lack of a decoalescence for both the *tert*-butyl and phenyl *quaternary* carbon resonances suggests strongly that benzyl rotation about the P–CH_2 bond is fast on the NMR time scale at 124 K. The observation of just three *tert*-butyl methyl NMR signals at 124 K suggests C_s symmetry. *tert*-Butyl rotation is slow, while libration

Chart I. Energy Profile for Ethyl Rotation about the P–CH_2 Bond in Di-*tert*-butylethylphosphine

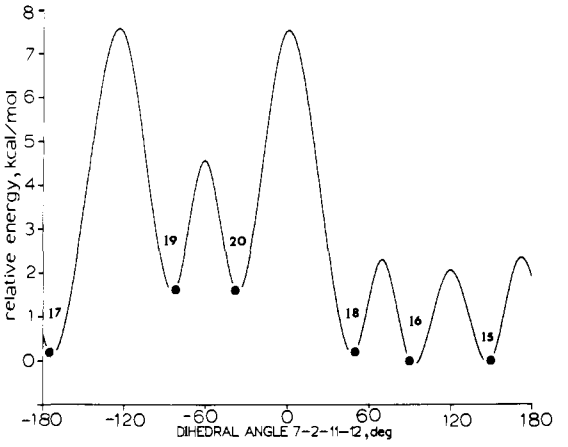

and benzyl rotation remain fast. The *tert*-butyl rotation barrier (ΔG^*) is 6.3 ± 0.3 kcal/mol at 138 K.

The $^{31}P\{^1H\}$ NMR spectrum (101.2 MHz) of **4** (5% v/v in vinyl chloride) at 260 K is a singlet (δ 33.7) and remains a singlet down to 110 K.

MM2 calculations were performed for **4**. Specific parameters for a P–benzyl group have not been developed. Therefore, we used sp^3–sp^3-P bond angle bending parameters (K_B = 400; θ = 120°) for the P–benzyl sp^2–sp^3-P bending parameters.[15] The torsional parameters for an sp^3–sp^3-P–sp^3 dihedral angle (V_1 = −0.05, V_2 = 0.0, and V_3 = 0.800)[15] were used for the P–benzyl sp^2–sp^3-P–sp^3 dihedral angle, and the torsional parameters for an sp^3–sp^3–sp^2-P dihedral angle (V_1 = 0.00, V_2 = 0.00, and V_3 = 1.10) were used for the P–benzyl sp^2–sp^2–sp^3-P dihedral angle.[15] Stretching parameters for the phenyl sp^2–sp^2 bonds (l_0 = 1.3937 Å; K_s = 8.0667 g cm s^{-2}) were added at run time as described in the documentation for the MM1 force field.[27]

The MM2 calculations suggest stereodynamics for **4** which are qualitatively similar to di-*tert*-butylethylphosphine with six chiral equilibrium conformations predicted (**21–26**). A perusal of selected MM2 structural parameters in Table VI will show that **21**, **23**, and **25** are diastereomeric, while there are three pairs of enantiomers (**21** and **22**, **23** and **24**, and **25** and **26**). A more comprehensive compilation of MM2 structural parameters can be found in supplemental Table IIIS. Enantiomers **21** and **22** which have a slight twist about the C11–P2 bond toward the lone pair are computed to be the most stable, while **23** and **24** are only slightly less stable (+0.04 kcal/mol; Table I). However, **25** is substantially less stable (+ 4.2 kcal/mol) than **21**. Thus, it is apparent that **25** and **26** will be present in concentrations too low

(27) Allinger, N. L. *QCPE* **1975**, 318.

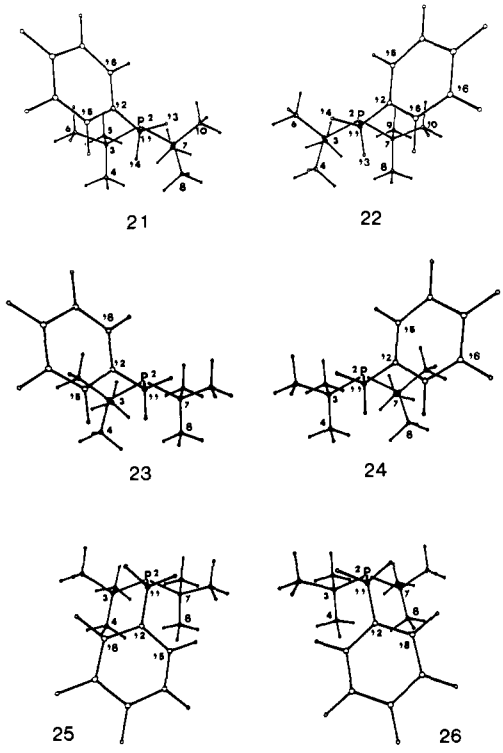

to be NMR-detectable, but **21–24** will all be present in essentially equal concentrations. It is apparent from the MM2 calculations that the phenyl group in **4** has a much greater preference for an orientation gauche to the lone pair (4.2 kcal/mol) than methyl of the ethyl group in **3** (1.6 kcal/mol). A similar trend is seen in benzyl and ethylamines.[2]

Dihedral angle driver calculations for both benzyl rotation (dihedral angle C7–P2–C11–C12) and *tert*-butyl rotation (angle C3–C2–C7–C8) produced the barriers in Table II. A perusal of Tables II and V and structures **21–26** will show that the stereodynamics of **4** are analogous to **3**. For **4**, there are four, essentially equally populated conformers (**21–24**) which can exchange via a series of low, DNMR-invisible barriers (**23** to **21** to **22** to **24** and vice versa) without involving *tert*-butyl rotation. Conformers **23** and **24** cannot interconvert directly. Exchange via **25** and **26** is highly unfavorable due to a high barrier to benzyl rotation. Thus, *slow tert*-butyl rotation on the NMR time scale at 124 K with *rapid* exchange among **21–24** will reflect time-averaged C_s symmetry in the NMR spectrum, as observed (Figures **11** and **12** in supplementary material).

Di-*tert*-butylisopropylphosphine (5). The ^1H NMR spectrum (250 MHz) of **5** (10% v/v in vinyl chloride) at 205 K shows a doublet at δ 1.19 (t-C_4H_9; $^3J_{PH}$ = 10.7 Hz) and the AM_6 part of an AM_6X spin system (i-C_3H_7P; X = ^{31}P; δ_A 1.85, δ_M 1.33, $^3J_{AM}$ = 7.7 Hz, $^2J_{AX}$ = 1.0 Hz, $^3J_{MX}$ = 11.0 Hz). Spectra of only the methyl region of **5** are shown in Figure 13 in the supplementary material. Below 160 K (Figure 13), the spectrum of the methyl region decoalesces and, at 119 K, is separated into a series of overlapping resonances. A decomposition of the theoretical simulation of the 119 K spectrum (see Figure 14 in supplementary material) shows three *tert*-butyl signals at δ 1.34 ($^3J_{PH}$ = 4.5 Hz), δ 1.26 ($^3J_{PH}$ = 13.8 Hz), and δ 1.16 ($^3J_{PH}$ = 14.8 Hz). At 119 K, the isopropyl subspectrum is simulated accurately by using an AM_6X spin system; i.e., isopropyl rotation about the P–CH bond is fast on the NMR time scale at 119 K. The symmetry reflected in the 119 K spectrum is C_s and is consistent with slow *tert*-butyl rotation on the NMR time scale, while all other rotations and any librations remain fast. The *tert*-butyl rotation barrier ($\Delta G^{\ddagger}$) is 6.7 ± 0.3 kcal/mol at 138 K. Below 119 K, the various resonances broaden into a meaningless spectrum.

The $^{13}C\{^1H\}$ DNMR spectra (62.9 MHz) of **4** (10% v/v in vinyl chloride) reveal the stereodynamics of both the *tert*-butyl *and* isopropyl groups. The spectrum of **4** at 262 K shows doublets

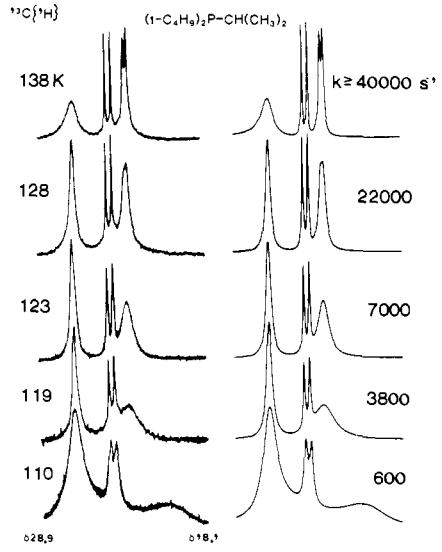

Figure 17. Experimental $^{13}C\{^1H\}$ DNMR spectra (62.9 MHz; left column) of the isopropyl region for di-*tert*-butylisopropylphosphine (**5**; 10% v/v in vinyl chloride). The lowest-field, broadened peak observed at 138 K is due to the *tert*-butyl methyl which is anti to the lone pair. Theoretical simulations (right column) are computed as a function of the rate of AG to GA isopropyl rotation (eq 1).

at δ 31.0 (t-C_4H_9 methyls; $^2J_{PC}$ = 13.7 Hz), δ 33.1 (t-C_4H_9 quaternary; $^1J_{PC}$ = 26.3 Hz), δ 23.5 (i-C_3H_7 methyls; $^2J_{PC}$ = 13.5 Hz), and δ 25.0 (i-C_3H_7 methine; $^1J_{PC}$ = 27.2 Hz). From 262 to 128 K, the *tert*-butyl methyls resonance decoalesces and is separated into *three* signals at 128 K (see Figures 15 and 16 in the supplementary material). Over the same temperature range, no other resonances decoalesce. The *tert*-butyl region of the spectrum is decomposed in Figure 16. The *tert*-butyl methyls show resonances at δ 26.7 ($^2J_{PC} \sim 5$ Hz; anti methyl; doublet coalesced due to short T_2), δ 32.8 ($^2J_{PC}$ = 15.0 Hz; gauche methyl), and δ 32.3 ($^2J_{PC}$ = 21.8 Hz; gauche methyl). The spectrum at 128 K suggests C_s symmetry and is consistent with slow *tert*-butyl rotation, while all other rotations and any librations are fast on the NMR time scale. This is consistent with the ^1H spectrum at 119 K (Figure 13 and 14 in the supplementary material). From a DNMR simulation of the $^{13}C\{^1H\}$ spectrum at 152 K, the $\Delta G^{\ddagger}$ value for *tert*-butyl rotation is 6.7 ± 0.4 kcal/mol.

Over the temperature range 138–110 K, the isopropyl methyls signal undergoes partial decoalescence. In the 138 K spectrum shown in Figure 17, the lowest field, exchange-broadened singlet (δ 26.7) is due to the *tert*-butyl methyl group which is anti to the lone pair (also see 138 K spectrum in Figure 15 in the supplementary material). Below 128 K, the isopropyl methyls resonance broadens significantly and is partially decoalesced at 110 K. The lowest temperature at which we could record a meaningful spectrum is 110 K. There is no decoalescence of the methine carbon doublet, which suggests strongly that the environment of the methine carbon does not change as a result of the DNMR-observed process associated with the isopropyl methyls. The subspectrum of the isopropyl methyls at 110 K (Figure 17) is simulated accurately by using an equally populated, *two-site*-exchange DNMR model with signals at δ 19.9 (assumed $^2J_{PC}$ = 5 Hz) and δ 26.6 (assumed $^2J_{PC}$ = 22 Hz) *and a first-order rate constant of 600 s^{-1}*. It is important to note that the two slow-exchange chemical shift values required for an accurate simulation at 110 K are *equidistant* from the time-averaged value at 138 K (δ 23.2), which does indeed speak for a simple two-site exchange. Excellent fits of the DNMR spectra from 110 to 138 K were achieved with the dynamic isopropyl methyls subspectrum superimposed upon the nondynamic *anti-tert*-butyl methyl and isopropyl methine subspectra (Figure 17). A decomposition of the theoretical simulation of the 110 K spectrum is shown in Figure 18.

The two-site decoalescence of the isopropyl methyls signal and the lack of any decoalescence of the methine carbon resonance

Table VII. Selected MM2 Structural Parameters for the Equilibrium Conformation of Di-*tert*-butylisopropylphosphine (**5**)[a]

parameter	conformation					
	27	**28**	**29**	**30**	**31**	**32**
dihedral angle, deg						
C3–P2–C7–C8	79.5	46.8	46.8	76.6	71.6	44.2
C4–C3–P2–C7	47.0	79.4	76.6	46.7	44.3	71.5
C3–P2–C11–C12	53.4	57.2	83.3	86.2	160.6	158.3
C7–P2–C11–C12	73.1	176.3	41.8	148.6	39.9	80.9
C7–P2–C11–C14	57.1	53.5	86.4	83.1	158.5	160.4
bond angle, deg						
C3–P2–C7	113.8	113.8	114.1	114.1	111.0	111.0
C3–P2–C11	108.3	112.2	106.2	111.8	107.3	109.9
C7–P2–C11	112.1	108.3	111.8	106.3	109.8	107.2
C12–C11–C14	108.4	108.4	109.6	109.5	103.1	103.1
bond length, Å						
P2–C3	1.846	1.843	1.849	1.841	1.862	1.856
P2–C7	1.843	1.846	1.841	1.849	1.856	1.862
P2–C11	1.839	1.839	1.839	1.839	1.849	1.849

[a] See supplemental Table IVS for a more comprehensive list of MM2 structural parameters.

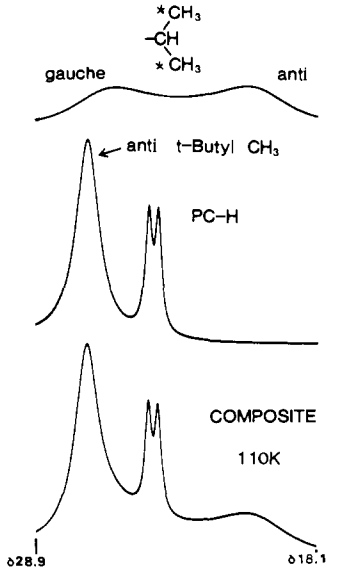

Figure 18. Decomposition of the theoretical simulation of the $^{13}C\{^1H\}$ spectrum of **5** at 110 K. Only the resonances due to the anti *tert*-butyl methyl and isopropyl groups are shown. The top subspectrum is due to the partially decoalesced isopropyl methyl signals.

are best assigned to isopropyl *rotation* which interchanges dominant, enantiomeric AG (anti/gauche) and GA rotamers (eq 1), while the GG conformer is present at a concentration too low to be NMR-detectable. It is satisfying to note that the ^{13}C NMR

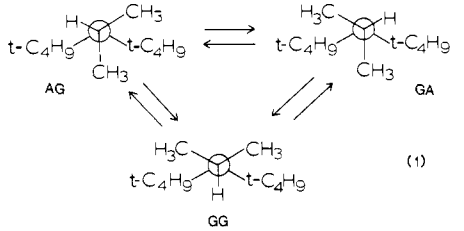

chemical shift difference between anti and gauche isopropyl methyl signals required in the two-site DNMR simulations ($\Delta\delta$ 6.7) is close to that for the anti and gauche *tert*-butyl methyl resonances of **5** at 128 K ($\Delta\delta \sim 6$ ppm). In principle, an AG to GA isopropyl rotation (eq 1) will induce a second decoalescence of the *tert*-butyl carbon resonances. The lack of any decoalescence at 110 K is consistent with a large rate of exchange (600 s^{-1}) and probably small $\Delta\delta$ values between diastereotropic *tert*-butyl carbons. The DNMR-determined barrier ($\Delta G^{\ddagger}$) for isopropyl rotation (4.8 ± 0.5 kcal/mol at 110 K) is lower than that for *tert*-butyl rotation (6.7 kcal/mol).

The $^{31}P\{^1H\}$ spectrum (101.2 MHz) of **5** (10% v/v in vinyl chloride) is a singlet (δ 45.9) at 262 K and remains a singlet to 110 K. There is precedent to suggest that significant populations of diastereomeric GG and AG (or GA) conformers (eq 1) would lead to a decoalescence of the ^{31}P signal due to slowing isopropyl rotation.[28] Thus, the ^{31}P singlet for **5** at 110 K is consistent with a strong preference for one type of conformer, i.e., the AG and GA enantiomers (eq 1).

MM2 calculations predict six equilibrium geometries for **5** (**27**–**32**). A perusal of Table VII and Supplemental Table IVS will show that **27**, **29**, and **31** are diastereomeric. There are three pairs of enantiomers (**27** and **28**; **29** and **30**; and **31** and **32**) with **29** and **30** and computed to be most stable. In **29**, all three alkyl

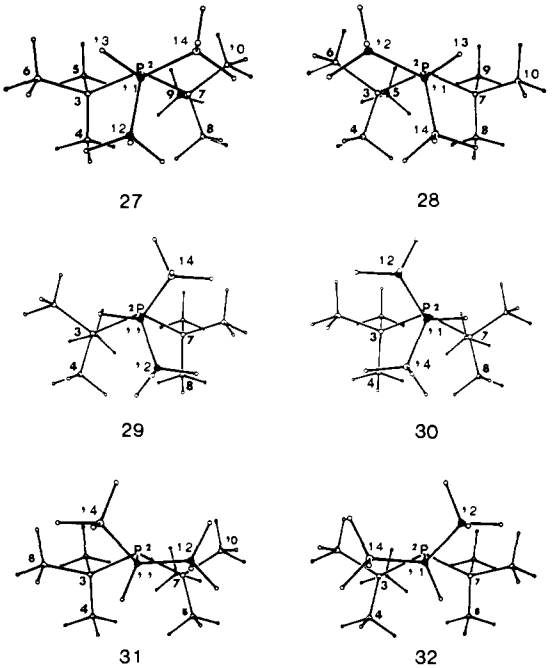

groups are twisted counterclockwise about the C–P bonds away from classical, staggered orientations (Table VII). In **27**, it is apparent that 1,3-dimethyl repulsions (C10/C14; C4/C12) are exacerbated and **27** is calculated to be 1.21 kcal/mol less stable than **29** (Table II). **31** is computed to be 3.5 kcal/mol less stable than **29**. It is apparent that the isopropyl methyl groups in **31** experience 1,3-dimethyl repulsions (C10/C12; C6/C14) with little opportunity to reduce these respulsions significantly via twisting. These increased 1,3-dimethyl repulsions in **31** are manifested in

(28) Dutasta, J. P.; Robert, J. B. *J. Chem. Soc., Chem. Commun.* **1975**, 747.

Chart II. Energy Profile for Isopropyl Rotation about the P–CH Bond in Di-*tert*-butylisopropylphosphine

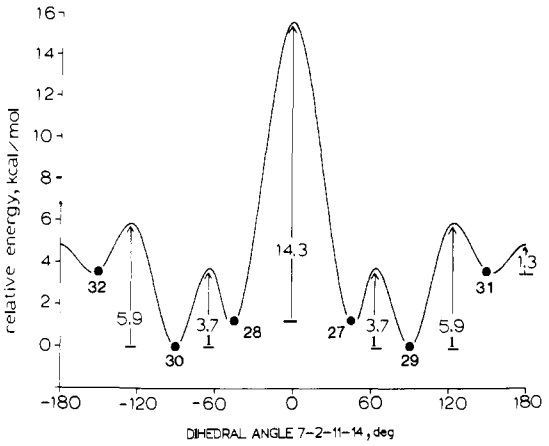

compressed MM2 bond angles C12–C11–C14 and C3–P2–C7 as compared to **29** (Table VII).

The MM2 calculations suggest that **27** and **28**, and especially **31** and **32**, will all be present at 110 K at concentrations too low to be NMR-detectable. The NMR spectrum at 110 K should reflect the essentially exclusive presence of the AG and GA conformers **29** and **30**. The spectrum at 110 K (Figures 17 and 18) is consistent with this prediction in that it rules out significant populations of GG conformers (**31** and **32**) but gives no information regarding the relative populations of **27** and **29** (or **28** and **30**).

Without invoking *tert*-butyl rotation, the six equilibrium conformations (**27**–**32**) can interconvert via a variety of isopropyl rotations, isopropyl librations, and *tert*-butyl librations. Using MM2-computed barriers (Table II), we constructed the energy profile shown in Chart II which is keyed to the C7–P2–C11–C14 dihedral angle. In perusing Chart II, remember that changes in dihedral angle C7–P2–C11–C14 are accompanied by geometric changes over the *whole* molecule. It is useful to use Chart II in conjunction with a careful examination of structures **27**–**32**. The most stable conformations **29** and **30** cannot racemize directly but must interconvert via **27** and **28** *or* via **31** and **32**. Eventual interconversion of **29** and **30** does interchange the isopropyl methyl groups between anti and gauche orientations to the lone pair. The MM2 barrier for the **29** to **27** libration is a low 3.7 kcal/mol, while the **27** to **28** rotation barrier is a much higher 14.3 kcal/mol. The **28** to **30** libration barrier is a low 2.5 kcal/mol. All the MM2 barriers for the other itinerary via **31** and **32** are much lower than 14.3 kcal/mol: **29** to **31** (5.9 kcal/mol), **31** to **32** (1.3 kcal/mol), and **32** to **30** (2.4 kcal/mol). Thus, it is apparent that the **29** to **30** exchange occurs preferentially via **31** and **32** as unstable intermediates, and it is this process that is observed in the $^{13}C\{^1H\}$ DNMR spectra below 128 K (Figure 17; $\Delta G^{\ddagger} = 4.8$ kcal/mol). The MM2 barrier (5.9 kcal/mol; Table II) is, once again, higher than the DNMR value.

MM2 barriers for C7 *tert*-butyl rotation (8.9 kcal/mol) and C3 *tert*-butyl rotation (8.0 kcal/mol) in **29** are predicted to be DNMR-visible but are higher than the DNMR value ($\Delta G^{\ddagger} = 6.7$ kcal/mol).

The stereodynamics of **5** are different from the ethyl (**3**) and benzyl (**4**) analogues. Whereas the preferred itineraries for exchange among the most stable conformers of **3** (Chart I) and **4** do not involve the least stable equilibrium geometries as intermediates, the preferred itinerary for interchange of the most stable conformers of **5** does involve the least stable equilibrium geometries as intermediates (Chart II).

Tri-*tert*-butylphosphine (6). The ^1H NMR spectrum (270 MHz) of **6** (10% v/v in vinyl chloride) at 260 K is a doublet (δ 1.27; $^3J_{PH} = 10.0$ Hz). Below 200 K, the doublet decoalesces and, at 150 K, is separated into two doublets at δ 1.36 ($^3J_{PH} = 3.1$ Hz; anti methyls) and at δ 1.22 ($^3J_{PH} = 13.4$ Hz; gauche methyls) with a respective area ratio of 1:2 (Figure 19 in the supplementary material). The 150 K spectrum reveals slow *tert*-butyl rotation

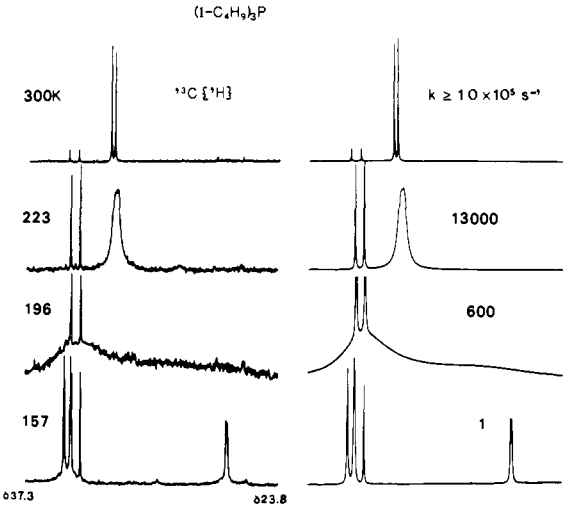

Figure 20. Experimental $^{13}C\{^1H\}$ DNMR spectra (62.9 MHz; left column) of tri-*tert*-butylphosphine (**6**; 10% v/v in vinyl chloride) and theoretical simulations as a function of the rate of *tert*-butyl rotation (k is defined in the Figure 4 caption).

about C–P bonds on the NMR time scale, rapid rotation of all methyl groups about C–C bonds, and C_{3v} symmetry. In light of the MM2 predictions of twisted *tert*-butyl groups in phosphines **1**–**5**, the C_{3v} symmetry reflected in the 150 K spectrum is presumably a time-averaged symmetry resulting from rapid libration. From a DNMR simulation at 180 K, the *tert*-butyl rotation barrier ($\Delta G^{\ddagger}$) is 8.9 ± 0.4 kcal/mol. Below 150 K, a differential broadening of the doublet at δ 1.22 occurs, but the spectra are broad, ill-defined, and not amenable to a meaningful analysis. The differential broadening may be due to a slowing of the libration process (vide infra).

The $^{31}P\{^1H\}$ NMR spectrum (101.2 MHz) of **6** (10% v/v in vinyl chloride) at 260 K is a singlet (δ 61.5) and remains a singlet down to 105 K.

The $^{13}C\{^1H\}$ NMR spectrum (62.9 MHz) of **6** (10% v/v in vinyl chloride) at 300 K shows doublets at δ 34.9 ($^1J_{PC} = 33.0$ Hz; quaternary carbons) and δ 32.8 ($^2J_{PC} = 13.3$ Hz; methyls). Below 200 K, the methyls resonance decoalesces and, at 157 K, is separated into two doublets at δ 26.5 ($^2J_{PC} = 4.7$ Hz; anti methyls) and δ 35.1 ($^2J_{PC} = 21.4$ Hz; gauche methyls) with a respective area ratio of 1:2 (Figure 20). At 157 K, the higher field component of the doublet at δ 35.1 overlaps the lower field component of the quaternary carbons doublet at δ 34.7. The quaternary carbons signal undergoes no decoalescence. This DNMR behavior corresponds exactly to the ^1H DNMR behavior (Figure 19), reflects C_{3v} symmetry at 157 K, and is assigned to slowing *tert*-butyl *rotation* ($\Delta G^{\ddagger} = 8.8 \pm 0.3$ kcal/mol at 196 K).

Below 157 K, the gauche methyls doublet (δ 35.1) undergoes an additional decoalescence and, at 112 K, is separated into two doublets of *equal area* at δ 35.4 ($^2J_{PC} = 29.9$ Hz) and δ 34.3 ($^2J_{PC} \cong 13$ Hz), while the anti methyls and quaternary carbons signals undergo no further decoalescence (Figure 21). In a decomposition of the theoretical simulation of the 112 K spectrum (Figure 22), the top subspectrum shows the nondynamic quaternary carbons signal, while the middle subspectrum clearly shows *three tert*-butyl methyl resonances. The spectral simulation at 112 K also required two very different $^2J_{PC}$ values for the gauche methyls resonances (29.9 Hz; 13 Hz) which speaks strongly for different orientations of the methyl groups with respect to the lone pair.[8] The observation of a single quaternary carbons signal and three different methyl resonances at 112 K is best rationalized in terms of NMR-exclusive enantiomeric equilibrium geometries having twisted *tert*-butyl groups and C_3 symmetry (see **33** and **34**). In the absence of any *tert*-butyl rotation, **33** and **34** can be racemized via a libration involving conrotatory torsions of all three *tert*-butyl groups. During this process, diastereotopic gauche methyls on a given *tert*-butyl group exchange between *different* sites, while the anti methyl exchanges between *equivalent* sites. The dec-

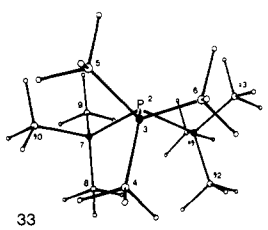

33

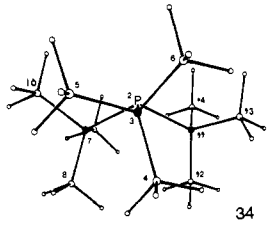

34

oalescence shown in Figure 21 is assigned to this libration process ($\Delta G^{\ddagger}$ = 5.9 ± 0.4 kcal/mol at 124 K). In contrast to phosphines **1–5**, the libration barrier in **6** is high enough to be DNMR-visible.

Although **6** is more sterically encumbered than phosphines **1–5**, MM2 calculations predict relatively simple stereodynamics. Two enantiomeric equilibrium geometries with C_3 symmetry are predicted (**33**, **34**; see Table VIII). All three *tert*-butyl groups undergo a 15.7° torsion away from C_{3v} symmetry. A comprehensive list of MM2 structural parameters can be found in supplemental Table VS. It is interesting to note that bond angles P2–C3–C4, P2–C7–C8, and P2–C11–C12 all open up to a relatively large 115.0° presumably in response to 1,3-dimethyl repulsions. These calculations are in substantial agreement with a previous MM1 force field study of **6** which predicted a 15.2° twist away from C_{3v} symmetry.[15] Semiempirical molecular orbital calculations predict a 36° twist,[16] and an electron diffraction study measured at 14° twist.[17]

An energy profile derived from a counterclockwise dihedral angle (C3–P2–C7–C8) driver calculation is shown in Figure 23. While the shape of this energy profile is similar to that for di-*tert*-butylphosphine (Figure 3), there are significant differences. The barriers for **6** are consistently much higher. The maxima near dihedral angles −180°, −60°, and 60° (Figure 23) which correspond to the *libration* barrier in **6** are much closer in magnitude to the maxima at −120°, 0°, and 120° which correspond to the *tert*-butyl *rotation* barrier. The MM2 *tert*-butyl rotation barrier (9.9 kcal/mol) compares favorably with the ^{1}H DNMR barrier ($\Delta G^{\ddagger}$ = 8.9 ± 0.4 kcal/mol at 180 K). The MM2 libration barrier (6.1 kcal/mol) is very close to the ^{13}C{^{1}H} DNMR barrier ($\Delta G^{\ddagger}$ = 5.9 ± 0.4 kcal/mol at 124 K).

The direct DNMR observation of libration and twisted *tert*-butyl groups in the C_3-symmetric **6** lends much credibility to the MM2 predictions of *tert*-butyl twisting in phosphines **1–5**.

Di-*tert*-butylphenylphosphine (7). The ^{1}H NMR spectrum (250 MHz) of **7** (10% v/v in tetrahydrofuran-d_8) at 305 K shows a doublet at δ 1.16 ($^3J_{PH}$ = 11.9 Hz; *t*-C_4H_9) and the AA'KLL' portion of an AA'KLL'X spectrum (C_6H_5P; X = ^{31}P) as shown in Figure 24 in the supplementary material. From a six-spin simulation using computer program UEAITR,[29] ^{1}H NMR parameters for phenyl were determined: δ_A 7.66 = $\delta_{A'}$ (ortho), δ_K 7.30 (para), δ_L 7.28 = $\delta_{L'}$ (meta), $^3J_{AX} = {}^3J_{A'X}$ = 7.3, $^4J_{LX} = {}^4J_{L'X}$ = 1.2, $^3J_{AL} = {}^3J_{A'L'}$ = 8.0, $^4J_{AK} = {}^4J_{A'K}$ = 2.0, $^3J_{KL} = {}^3J_{KL'}$ = 7.0 Hz.

The spectrum at 305 K reveals isochronous ortho protons and is consistent with rapid phenyl rotation on the NMR time scale. Below 250 K, the ortho protons resonance undergoes a clear-cut, decoalescence (Figure 24). At 175 K, the phenyl group gives an AGKLMX spectrum (X = ^{31}P): δ_A 7.80 (ortho; $^3J_{AX}$ = 1.5 Hz), δ_G 7.53 (ortho; $^3J_{GX}$ = 12.0 Hz), δ_K 7.38 (para), δ_L 7.38 (meta, $^4J_{LX} \cong$ 0.3 Hz), δ_M 7.34 (meta, $^4J_{MX}$ = 2.0 Hz), $^3J_{AL}$ = 7.0, $^3J_{GM}$ = 7.0 Hz. All other $^3J_{HH}$, $^4J_{HH}$, and $^5J_{HH}$ values are 7.0, 1.5–2.0, and 0.1 Hz, respectively.[29]

The 175 K spectrum shows anisochronous ortho protons and *slow phenyl rotation on the NMR time scale.* The very different $^3J_{AX}$ (1.5 Hz) and $^3J_{GX}$ (12.0 Hz) values for coupling of the ortho protons to phosphorus strongly suggest that the proton at δ_A 7.80 is anti to the phosphorus lone pair and the proton at δ_G 7.53 is syn. Letter designations for the various ^{1}H chemical shift assignments are shown on **35**. A similar but attenuated trend is seen in the $^4J_{LX}$ and $^4J_{MX}$ values for the meta protons (vide supra).

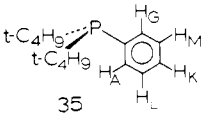

35

The 175 K spectrum suggests C_s molecular symmetry with the phenyl plane bisecting the *tert*-butyl groups (**35**). It is apparent that the process being observed is essentially a 2-fold phenyl rotation during which H_A and H_G exchange sites (**35**). *Over the temperature range 305-175 K, the tert-butyl resonance undergoes no changes; i.e., tert-butyl rotation is fast on the NMR time scale at 175 K.* The simulations of the 175 and 305 K spectra show that an AGKLMX to GAKMLX chemical shift exchange is occurring. We used a simplified three-spin/two-configuration DNMR model (i.e., ALX to GMX; see **35**) to simulate the decoalescence of the *ortho protons only* (Figure 24). From the simulation at 223 K, the phenyl rotation barrier ($\Delta G^{\ddagger}$) is 10.2 ± 0.5 kcal/mol.

The ^{31}P{^{1}H}NMR spectrum of **7** (10% v/v in tetrahydrofuran-d_8) at 305 K is a singlet (δ 40.2) and does not change down to 175 K. In vinyl chloride as the solvent, the spectrum remains a singlet down to 119 K.

The ^{13}C{^{1}H} NMR spectrum (62.9 MHz) of **7** (10% v/v in tetrahydrofuran-d_8) at 330 K shows doubets for *tert*-butyl at δ 30.8 (CH_3; $^2J_{PC}$ = 14.9 Hz) and δ 32.3 (quaternary; $^1J_{PC}$ = 24.1 Hz). The phenyl group gives doublets at δ 128.1 (meta; $^3J_{PC}$ = 8.5 Hz), δ 129.5 (para; $^4J_{PC}$ = 1.4 Hz), δ 137.2 (ortho; $^2J_{PC}$ = 23.2 Hz), and δ 138.2 (quaternary; $^1J_{PC}$ = 24.8 Hz). Below 280 K, the ortho carbons resonance decoalesces and, at 181 K, is separated into two doublets of equal area at δ 134.5 ($^2J_{PC}$ = 5.5 Hz) and δ 139.8 ($^2J_{PC}$ = 49.9 Hz), showing very different $^2J_{PC}$ values (Figure 25). The meta carbons resonance also decoalesces into two doublets of equal area at δ 128.1 ($^3J_{PC} \cong$ 0.3 Hz) and δ 128.5 ($^3J_{PC}$ = 16.7 Hz) also with very different $^3J_{PC}$ values (Figure 25). The phenyl quaternary and para carbons signals remain unchanged over the 330–181 K temperature range. *Over the same temperature range, the tert-butyl resonances remain sharp and unchanged.* The 181 K spectrum is consistent with slow phenyl rotation, fast *tert*-butyl rotation, and corresponds exactly to the ^{1}H DNMR data (vide supra). Consistent with previous studies,[30] the ortho carbon of **7** which gives the signal at δ 139.8 with the larger $^2J_{PC}$ value (49.9 Hz) is oriented syn to the lone pair and that giving the signal at δ 134.5 ($^2J_{PC}$ = 5.5 Hz) is anti. The meta carbon of **7** which gives the resonance at δ 128.5 ($^3J_{PC}$ = 16.7 Hz) is syn to the lone pair.[30] All these data are consistent with C_s molecular symmetry (**35**).

DNMR simulations of the ortho and meta carbons resonances were achieved in each case by using two-spin (^{13}C, ^{31}P)/two-configuration models with the nondynamic quaternary and para carbon signals included (Figure 25). The phenyl rotation barrier ($\Delta G^{\ddagger}$) is 10.5 ± 0.3 kcal/mol at 228 K which is in agreement with the ^{1}H DNMR value (10.2 ± 0.5 kcal/mol at 223 K).

Below 170 K, decoalescence of both the ^{1}H and ^{13}C{^{1}H} methyl resonances of **7** (10% v/v in vinyl chloride) occurs. The *tert*-butyl ^{1}H NMR doublet (δ 1.16; $^3J_{PH}$ = 11.9 Hz) observed at 180 K is decoalesced at 115 K into three doublets at δ 1.32 ($^3J_{PH}$ = 5.5 Hz), δ 1.31 ($^3J_{PH}$ = 14.0 Hz), and δ 0.83 ($^3J_{PH}$ = 15.7 Hz) as shown in Figure 26 in the supplementary material. The observation of just three methyl signals at 115 K is consistent with slow *tert*-butyl rotation and presumably reflects time-averaged C_s symmetry resulting from rapid libration (vide supra). From a DNMR simulation at 140 K, the *tert*-butyl rotation barrier ($\Delta G^{\ddagger}$) is 6.5 ± 0.4 kcal/mol).

The ^{13}C{^{1}H} NMR spectrum (62.9 MHz) of the *tert*-butyl region of **7** (10% v/v in vinyl chloride) at 252 K shows the quaternary carbons doublet at δ 32.1 ($^1J_{PC}$ = 24.1 Hz) and the methyls doublet at δ 29.6 ($^2J_{PC}$ = 15.0 Hz). Below 170 K, the methyls signal decoalesces (Figure 27). As determined from a

(29) Johannesen, R. B.; Ferretti, J. A.; Harris, R. K. *QCPE* **1985**, *188*.

(30) (a) Sorenson, S.; Hansen, R. S.; Jakobsen, H. J. *J. Am. Chem. Soc.* **1972**, *94*, 5902. (b) Jakobsen, H. J.; Begtrap, M. *J. Mol. Spectrosc.* **1971**, *40*, 276.

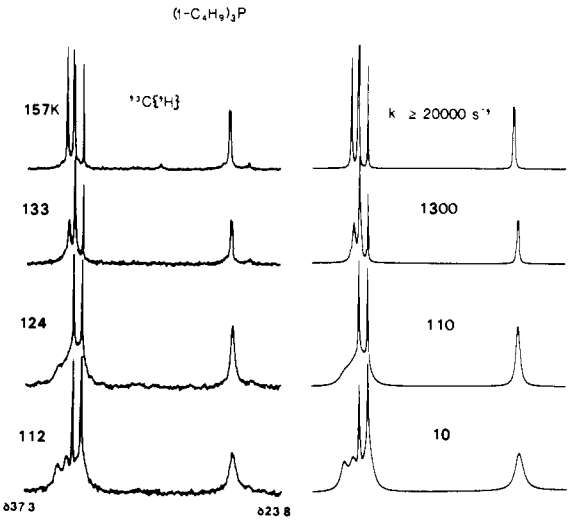

Figure 21. Experimental $^{13}C\{^1H\}$ DNMR spectra (62.9 MHz; left column) of tri-*tert*-butylphosphine (**6**; 10% v/v in vinyl chloride) and theoretical simulations as a function of the rate of libration between the C_3-symmetric conformers.

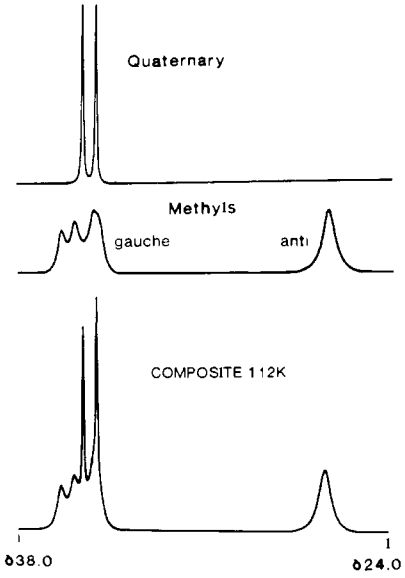

Figure 22. Decomposition of the theoretical simulation of the $^{13}C\{^1H\}$ spectrum of **6** at 112 K. The middle subspectrum is due to the methyl carbons.

Table VIII. Selected MM2 Structural Parameters for the Equilibrium Conformations of Tri-*tert*-butylphosphine (**6**)[a]

parameter	conformation 33	conformation 34
dihedral angle, deg		
C3-P2-C7-C8	78.9	47.5
C4-C3-C11	78.9	47.6
C7-P2-C11-C12	78.9	47.4
bond angle, deg		
C3-P2-C7	111.9	111.9
C3-P2-C11	111.9	111.9
C7-P2-C11	111.9	111.9
bond length, Å		
P2-C3	1.856	1.856
P2-C7	1.856	1.856
P2-C11	1.856	1.856

[a] See supplemental Table VS for a more comprehensive list of MM2 structural parameters.

complete DNMR line shape simulation which incorporates the *nondynamic* quaternary carbons doublet, the spectrum of the methyl groups at 119 K shows three doublets at δ 26.7 ($^2J_{PC}$ = 6.5 Hz), δ 32.2 ($^2J_{PC} \cong$ 19 Hz), and δ 31.9 ($^2J_{PC} \cong$ 21 Hz). The

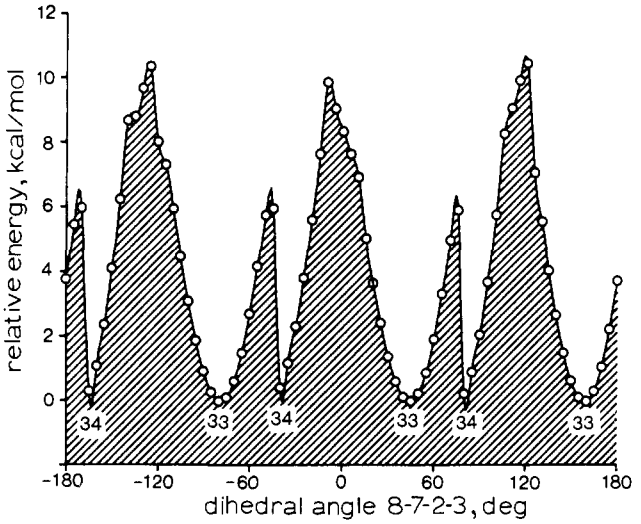

Figure 23. MM2 energy profile derived from a dihedral angle driver calculation for tri-*tert*-butylphosphine (**6**). Dihedral angle C3–P2–C7–C8 (see **33**) is changed in 5° counterclockwise increments looking down the C7–P2 bond.

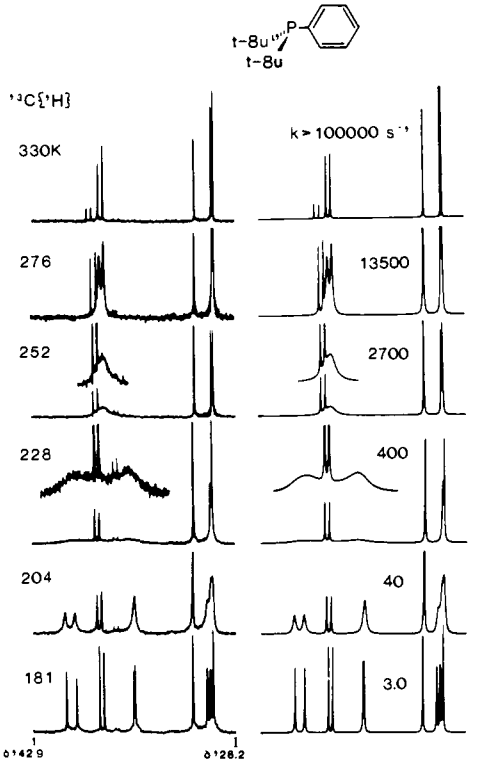

Figure 25. Experimental $^{13}C\{^1H\}$ DNMR spectra (62.9 MHz; left column) of the phenyl region only for di-*tert*-butylphenylphosphine (**7**; 10% v/v in tetrahydrofuran-d_8) and theoretical simulations as a function of 2-fold phenyl rotation (k is the first-order rate constant for a single rotation).

119 K spectrum shows slow *tert*-butyl rotation and time-averaged C_s symmetry due to fast libration. From a DNMR simulation at 138 K, the *tert*-butyl rotation barrier ($\Delta G^{\ddagger}$) is 6.2 ± 0.4 kcal/mol.

Over the temperature range 170–115 K, the ^1H and $^{13}C\{^1H\}$ spectra of the phenyl group undergo no further changes. At 119 K, the $^{31}P\{^1H\}$ spectrum of **7** is a singlet. The NMR data at 119 K suggest time-averaged C_s symmetry (e.g., **35**) with phenyl rotation ($\Delta G^{\ddagger}$ = 10.5 kcal/mol) substantially more restricted than *tert*-butyl rotation ($\Delta G^{\ddagger}$ = 6.3 kcal/mol) and very facile, DNMR-invisible libration.

The MM2 force field predicts two enantiomeric equilibrium geometries for **7** (eq 2; **36** and **37**).[31] Table IX and supplemental

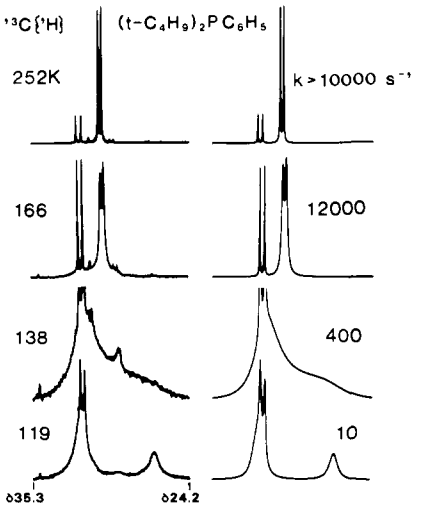

Figure 27. Experimental $^{13}C\{^1H\}$ DNMR spectra (62.9 MHz; left column) of the *tert*-butyl region only of di-*tert*-butylphenylphosphine (**7**; 10% v/v in vinyl chloride) and theoretical simulations as a function of the rate of *tert*-butyl rotation (k is defined in the Figure 4 caption).

Table IX. Selected MM2 Structural Parameters for the Equilibrium Conformations of Di-*tert*-butylphenylphosphine (**7**)[a]

parameter	conformation		
	36	**37**	**38** ‡
dihedral angle, deg			
C3–P2–C7–C8	39.5	69.1	83.4
C4–C3–P2–C7	69.1	39.5	69.5
C3–P2–C11–C12	68.8	55.0	163.0
bond angle, deg			
C3–P2–C7	115.4	115.4	114.8
C3–P2–C11	105.1	107.6	109.8
C7–P2–C11	107.8	105.2	106.7
bond length, Å			
P2–C3	1.839	1.835	1.848
P2–C7	1.835	1.839	1.856
P2–C11	1.809	1.809	1.840

[a] See supplemental Table VIS for a more comprehensive list of MM2 structural parameters.

Table VIS will show that **36** and **37** have C_1 symmetry and are enantiomeric. In **36**, phenyl is twisted 7° counterclockwise away from C_s symmetry, and both *tert*-butyl groups also undergo counterclockwise twists. It is apparent once again that the *tert*-butyl groups twist in response to *syn*-1,3-dimethyl repulsions, and the conformational preference of phenyl is then determined in turn by the orientation of the *tert*-butyl moieties.

tert-Butyl rotation and libration were studied by using the dihedral angle driver method (∠C3–P2–C7–C8). Conformer **36** can be converted to **37** via *libration* which involves small torsions about all three C–P bonds. The MM2 barrier for this libration is a very low, DNMR-invisible 1.0 kcal/mol. Alternatively, **36** can be converted to **37** via a counterclockwise *rotation* of the C7 *tert*-butyl *in conjunction with* small clockwise torsions of the other two groups. The MM2 barrier for this *rotation* is a DNMR-visible 7.0 kcal/mol which, once again, is higher than the DNMR-measured value (6.3 kcal/mol; Table I). The C_s symmetry reflected in the $^{13}C\{^1H\}$ and ^1H spectra of **7** at 115 K (Figures 26 and 27) is indeed consistent with slow *tert*-butyl rotation and fast libration on the NMR time scale.

Phenyl rotation was studied by driving the dihedral angle C7–P2–C11–C12 in clockwise and counterclockwise directions. As compared to the *tert*-butyl driver calculation, there is more hysteresis in the phenyl rotation energy profiles, and the results might be viewed with more caution. However, there is a good qualitative correlation with the experimental DNMR data. For example, the libration barrier is predicted to be a DNMR-invisible 3.5 kcal/mol. The *tert-butyl* driver calculation gives 1.0 kcal/mol. The barrier to phenyl rotation is computed to be 14.0 kcal/mol, while the DNMR value is 10.5 kcal/mol. The MM2 force field correctly predicts the barrier ordering for *tert*-butyl and phenyl rotation. The MM2 transition state for phenyl rotation is **38** which is shown in eq 2 and also shown separately below with pertinent atoms numbered. **38** does not have true C_s symmetry, but it is close (Table IX and supplemental Table VIS). Bond angles C5–C3–C6 (100.8°) and C9–C7–C10 (102.8°) in **38** are compressed as compared to **36** (107.2°; 106.4°), reflecting increased nonbonded repulsions in **38** between ortho protons (H16; H18) and the C6 and C10 methyls (see separate structure **38**). The MM2-calculated H15/H16 (1.89 Å) and H17/H18 (1.93 Å) distances in **38** are much shorter than the respective distances in **36** (4.00 Å; 3.96 Å).

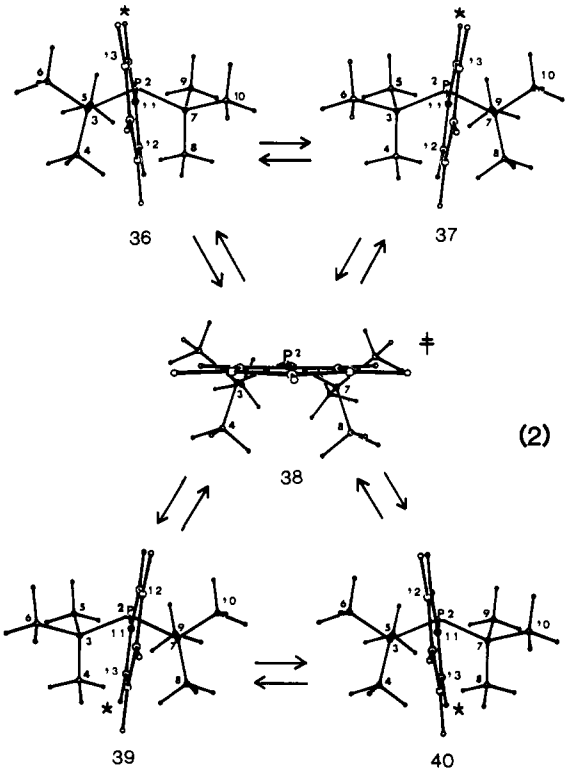

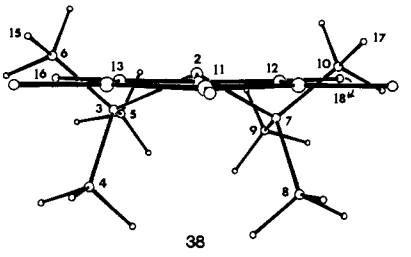

Thus, the stereodynamics of **7** would seem to be adequately summarized in eq 2. Equilibrium conformers **36** and **37** (or **39** and **40**) can racemize via low-barrier, DNMR-invisible librations. A counterclockwise phenyl *rotation* starting at **36** will produce transition-state **38** and eventually **39**. During this process, ortho carbons C12 and C13 exchange between positions syn and anti to the lone pair (eq 2). It would appear that the relatively high phenyl rotation barrier (10.5 kcal/mol) is due in small part to enhanced *syn*-1,3-dimethyl repulsions involving the *tert*-butyl groups in **38** (~1 kcal/mol) and in large part to repulsions between ortho protons and proximate methyl groups in **38** (~10 kcal/mol). *tert*-Butyl rotation occurs with a lower, albeit DNMR-visible barrier (6.3 kcal/mol). The ^1H and $^{13}C\{^1H\}$ spectra of **7** at 115 K reflect a time-averaged C_s symmetry consistent with slow *tert*-butyl and phenyl rotation on the NMR time scale, while all libration processes remain fast.

(31) Stretching parameters for phenyl were added at run time in the same manner as described for **4**. We assigned a value of 0.05 g cm s^{-2} to P-sp^2 out-of-plane bending parameter.

Table X. Typical FT NMR Acquisition Parameters

parameter	^1H	$^{13}C\{^1H\}$	$^{31}P\{^1H\}$
total scans	32	240	32
sweep width, Hz	3000	13000	10000
Fourier no.	16K	16K	8K
cycle time, s	3.0	1.5	1.5
pulse width, μs	2	9	9

Experimental Section

The variable-temperature 101.2-MHz $^{31}P\{^1H\}$ and 62.9-MHz $^{13}C\{^1H\}$ pulsed FT NMR spectra were recorded on a Bruker WM250 NMR system at the University of Vermont using a custom-built cold nitrogen gas delivery system, modified superconducting magnet cavity, and Bruker BVT-1000 temperature control unit. Temperature measurement is accurate to ±3 K for ^1H spectra and ±4 K for $^{13}C\{^1H\}$ and $^{31}P\{^1H\}$ spectra. Due to the error in temperature measurement, we do not report $\Delta H^{\ddagger}$ and $\Delta S^{\ddagger}$ values. The variable-temperature 270-MHz ^1H FT NMR spectra were recorded on a Bruker HX270 NMR system at the NSF Regional Instrumentation Center, Yale University. All spectra were obtained by using quadrature-phase detection. Typical acquisition parameters are listed in Table X. All NMR samples were sealed after a minimum of three freeze–pump–thaw cycles using a vacuum below 0.1 torr.

Certain phosphines were synthesized by using literature procedures. Others were purchased. All reactions were performed under nitrogen and manipulated inside nitrogen-flushed glovebags. All solvents used in synthesis and workup were either thoroughly degassed or distilled under nitrogen. Diethyl ether and tetrahydrofuran were freshly distilled from sodium and benzophenone ketal.

Di-*tert*-butylphosphine (1),[32] **di-*tert*-butylmethylphosphine (2)**,[33] **di-*tert*-butylethylphosphine (3)**,[34] **di-*tert*-butylbenzylphosphine (4)**,[35] and **di-*tert*-butylisopropylphosphine (5)**[34] are all known compounds and were synthesized by literature procedures: NMR data, see text.

Tri-*tert*-butylphosphine (6) and **di-*tert*-butylphenylphosphine (7)** were purchased from Strem Chemicals Co. and used without further purification: NMR data, see text.

Acknowledgment. We are grateful to the National Science Foundation for financial support (Grant CHE-8024931 and CHE-8306876) and to the University of Vermont Academic Computing Center for outstanding computational support.

Supplementary Material Available: Figures 1, 2, 5, 6, 9–16, 19, 24, and 26 of NMR spectra (**1–6**) and Tables IS, IIS, IIIS, IVS, VS, and VIS of bond angles and bond lengths (**1–7**) (40 pages). Ordering information is given on any current masthead page.

(32) Hoffmann, H.; Schellenbeck, P. *Chem. Ber.* **1966**, *99*, 1134.
(33) Crofts, P. C.; Parker, D. M. *J. Chem. Soc. C* **1970**, 332.
(34) Hoffman, H.; Schellenbeck, P. *Chem. Ber.* **1967**, *100*, 692.
(35) Stewart, A. P.; Trippett, S. *J. Chem. Soc. C* **1970**, 1263.

Structure and Conformations of 4-Chloro-1-butanol: Electron-Diffraction Evidence for Internal Hydrogen Bonding

Otto Bastiansen, Liv Fernholt, Kenneth Hedberg,* and Ragnhild Seip

Contribution from the Department of Chemistry, University of Oslo, P.B. 1033, Blindern 0315, Oslo 3, Norway. *Received July 15, 1985*

Abstract: Internal hydrogen bonding is generally believed to occur in the free molecules of substances that have suitable, properly oriented, donor and acceptor groups, as in 2-chloro- or 2-fluoroethanol. However, such bonding is difficult to establish by purely structural means because the orientation of the skeletal atoms is also influenced by a "gauche effect" when the donator and acceptor groups are separated by only one skeletal torsion angle. Accordingly, we have investigated the structure of 4-chloro-1-butanol, a molecule in which any gauche effect should be minimal, for evidence of internal hydrogen bonding. If rotation about each C–C bond is assumed to generate three potential energy minima, this molecule has 14 conformers that are characterized by different distances between the heavy atoms, only one of which has the Cl and O atoms within hydrogen-bonding distance. Since it is not possible to determine the composition of such a complicated mixture of conformers by electron diffraction, calculations from molecular mechanics were used to predict a composition *exclusive of any assumed contribution to the energy from hydrogen bonding.* Refinement of models in which the mole fraction of the hydrogen-bonded conformer was allowed to adjust led to large increases over that predicted from molecular mechanics. We take these results as strong evidence for the existence of internal hydrogen bonding. Values for the structural parameters and conformational composition are presented.

The problem of internal hydrogen bond formation is an intriguing one. Evidence for the existence of such bonds is found in the structures of many molecules in which internal rotation plays a role, such as glycol and glycerol,[1] and in the 2-haloethanols, molecules of particular interest in connection with the work to be described here. In the cases of 2-chloro-[1-4] and 2-bromoethanol,[2,5] for example, the lower energy of the gauche ($\phi \simeq 55°$) forms relative to the anti ($\phi \simeq 180°$) stands in contrast to the relative energies of these forms in the corresponding 1,2-dihaloethanes[5-8] in which the anti form is the lower energy one and has been attributed to the stabilizing effect of O–H···X bond formation. This satisfying picture is clouded by the results for 2-fluoroethanol[9,10] and 1,2-difluoroethane:[6,11,12] the more stable form for the former is of course gauche; the latter, however, is not the expected anti but is also gauche.

The stability of the gauche forms of such 1,2-disubstituted compounds with electronegative substituents has been accounted

*On sabbatical leave. Permanent address: Department of Chemistry, Oregon State University, Corvallis, Oregon 97331.

(1) Bastiansen, O. *Acta Chem. Scand.* **1949**, *3*, 415.
(2) Azrak, R. G.; Wilson, E. B., Jr. *J. Chem. Phys.* **1970**, *52*, 5299.
(3) Almenningen, A.; Bastiansen, O.; Fernholt, L.; Hedberg, K. *Acta Chem. Scand.* **1971**, *25*, 1946.
(4) Almenningen, A.; Fernholt, L.; Kveseth, K. *Acta Chem. Scand.* **1977**, *A31*, 297.
(5) Ainsworth, J.; Karle, J. *J. Chem. Phys.* **1952**, *20*, 425.
(6) Brunnvoll, J., Licenciate thesis, Norwegian Technical University, Trondheim, 1962.
(7) (a) Kveseth, K. *Acta Chem. Scand.* **1974**, *A28*, 482. (b) Kveseth, K. *Ibid.* **1975**, *A29*, 307.
(8) Fernholt, L.; Kveseth, K. *Acta Chem. Scand.* **1978**, *A32*, 63.
(9) Buckton, K. S.; Azrak, R. G. *J. Chem. Phys.* **1970**, *52*, 5652.
(10) Hagen, K.; Hedberg, K. *J. Chem. Phys.* **1973**, *95*, 8263.
(11) van Schaick, E. J. M.; Geise, H. J.; Mijlhoff, F.; Reves, G. *J. Mol. Struct.* **1972**, *16*, 23.
(12) Friesen, D.; Hedberg, K. *J. Am. Chem. Soc.* **1980**, *102*, 3887.

0002-7863/85/1507-7836$01.50/0